Evolution of Neogene volcanism and stress patterns in the glaciated West Antarctic Rift, Marie Byrd Land, Antarctica

Timothy S. Paulsen and Terry J. Wilson

Journal of the Geological Society 2010; v. 167; p. 401-416
doi: 10.1144/0016-76492009-044

Journal of the Geological Society, London, Vol. **167**, 2010, pp. 401–416. doi: 10.1144/0016-76492009-044.

Evolution of Neogene volcanism and stress patterns in the glaciated West Antarctic Rift, Marie Byrd Land, Antarctica

TIMOTHY S. PAULSEN[1]* & TERRY J. WILSON[2]

[1]*Department of Geology, University of Wisconsin Oshkosh, 800 Algoma Blvd., Oshkosh, WI 54901, USA*

[2]*Byrd Polar Research Center and School of Earth Sciences, Ohio State University, 108 Scott Hall, 1090 Carmack Road Columbus,OH 43210, USA*

**Corresponding author (e-mail: paulsen@uwosh.edu)*

Abstract: The orientations and ages of polygenetic volcano chains, elongate volcano edifices, and elongate summit calderas in Marie Byrd Land, Antarctica, are analysed to determine stress directions during volcanism and coeval glaciation across the West Antarctic Rift. Initiation of volcanism *c*. 36–34 Ma and major polygenetic volcanism beginning *c*. 14 Ma are broadly coeval with establishment of significant ice volumes in West Antarctica. Middle–Late Miocene volcanism occurred primarily along roughly north–south volcano chains, whereas latest Miocene–Pleistocene volcanism had a strong east–west preferred orientation across the spatial extent of the province. Anisotropic stress conditions controlled both phases of volcanism, and a rapid rotation in the maximum horizontal stress direction from north–south to east–west occurred as early as *c*. 6 Ma. Glacial loading and unloading appears to have facilitated volcanism in Marie Byrd Land, but ice margin reconstructions make it unlikely that stress field rotation is a result of flexural stresses imposed by glacial loading cycles. The east–west orientation of latest Miocene to Pleistocene maximum horizontal stress is parallel to the absolute motion of the Antarctic plate for the past 6 Ma, and the north–south to east–west stress field rotation coincides with changes in Antarctic–Pacific Ridge spreading and Pacific basin tectonic events associated with plate reorganization.

The West Antarctic Rift system transects the Antarctic continent and is the only rift system on Earth covered by a continental-scale ice sheet (the West Antarctic Ice Sheet). Rifting commenced during Mesozoic breakup of Gondwanaland and has continued episodically into the Neogene (Cooper *et al*. 1987; Cande *et al*. 2000; Henrys *et al*. 2007; Sutherland 2008). Antarctic glaciation has temporally and spatially overlapped with rifting since the inception of Antarctic ice sheets *c*. 34 Ma (Zachos *et al*. 2001). Little is known about the Neogene to contemporary geodynamic evolution of the rift system, as the extensive ice cover hampers field studies, geophysical data are sparse, there has been little drilling, and seismic events of sufficient magnitude for focal mechanism solutions have not been recorded (Reading 2006) .

Antarctica contains widespread Neogene to active volcanoes, which can provide an important source of stress data (Nakamura 1977; Nakamura *et al*. 1977). This study focuses on the Neogene stratovolcanoes and shield volcanoes exposed as nunataks above the West Antarctic Ice Sheet in Marie Byrd Land, West Antarctica. Both mantle plumes and decompression melting of a fertile mantle during minor structural reactivation of crustal structures have been invoked to produce the magma of the Marie Byrd Land volcanic province, and of the broadly coeval Cenozoic McMurdo magmatic province in the western portion of the West Antarctic Rift system (LeMasurier & Rex 1989; LeMasurier & Thomson 1990; Behrendt *et al*. 1992; Panter *et al*. 1994; Rocchi *et al*. 2002, 2006; Finn *et al*. 2005). Regardless of the processes associated with melt generation, fracture processes controlled the ascent of magma to the surface to produce the widespread surface volcanism across the Marie Byrd Land province. In this contribution we focus on the conditions associated with the fracture of the crust to bring magma to the surface to form polygenetic volcanoes. Because the stresses in the crust, both regional and local, control rock fracture, we can derive information about crustal stress regimes from the volumes, alignments, shapes and orientations of magma conduits and their surface expressions, namely volcanoes and calderas.

The unusual pattern of the Marie Byrd Land volcanoes, which appear to define north–south and east–west chains (Figs 1 and 2), has long been attributed to lithospheric structural control on volcanism (e.g. LeMasurier & Rex 1989; Siddoway 2008). Here we systematically examine the volcano alignments, volcano shapes, volcano flank vent distributions, and caldera shapes (e.g. Fig. 3a and b), which are all established indicators of crustal stress directions at the time the volcanoes formed (Nakamura 1977; Nakamura *et al*. 1977; Bosworth *et al*. 2003). We apply a 'reliability ranking' to the volcano stress indicators, to help take into account the obstacles to stress analysis in the region, which include the extensive ice cover and the reconnaissance nature of field mapping and age dating at most volcanoes. A new compilation of available age data allows us to evaluate the stress indicators relative to 'age windows' to assess whether stresses have changed in orientation through the Neogene.

Stress directions are then evaluated in the context of potential controls on the intraplate continental stresses in Marie Byrd Land. Both tectonic stresses arising from plate-boundary forces and regional stresses arising from glacial loading and unloading as a result of West Antarctic Ice Sheet response to climate change are expected to be important. Therefore, we compare our stress results with known events affecting the Antarctic plate and with important time periods in the evolution of the West Antarctic Ice Sheet. Although event chronology remains

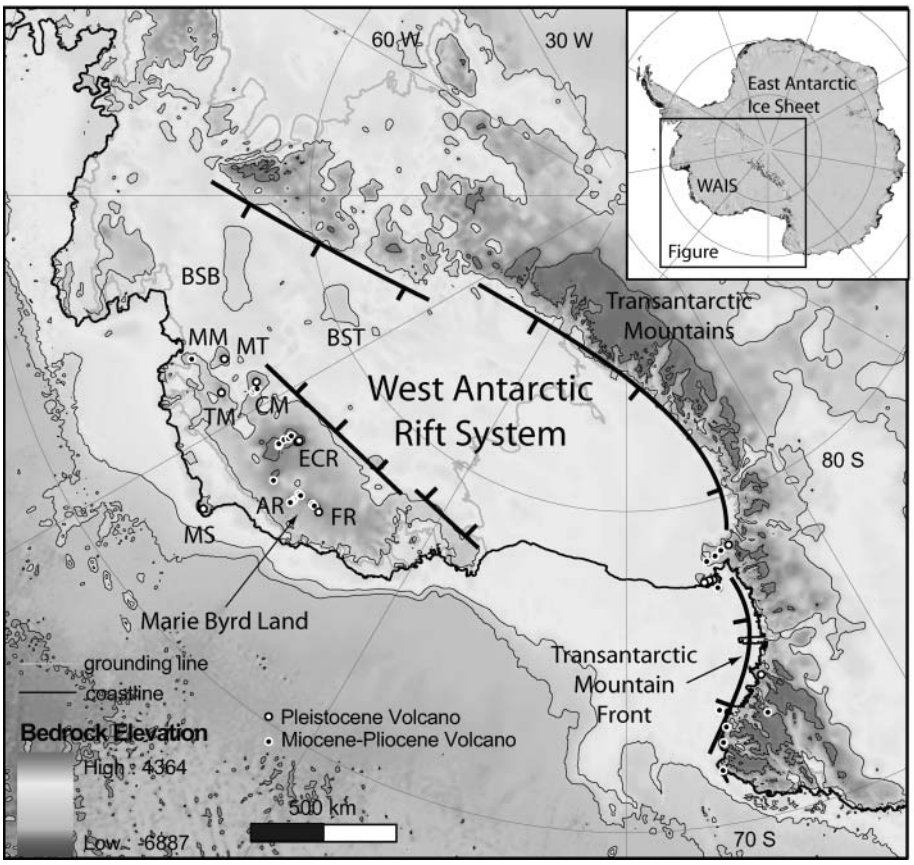

Fig. 1. Bed elevation map of Antarctica showing the location of the glaciated Marie Byrd Land area with respect to the West Antarctic Rift system and the Transantarctic Mountains rift flank uplift. (Note the major volcanoes in Marie Byrd Land, as well as the east–west elongated high topography of Marie Byrd Land and its parallelism to the rift system.) Inset shows the location of the figure with respect to Antarctica, as well as the location of the East and West Antarctic ice sheets. Bed elevation data from Lythe *et al*. (2000). Contour interval 1500 m. AR, Ames Range; BSB, Byrd Subglacial Basin; BST, Bentley Subglacial Trough; CM, Crary Mountains; ECR, Executive Committee Range; FR, Flood Range; MM, Mount Murphy; MS, Mount Siple; MT, Mount Takahe; TM, Toney Mountain.

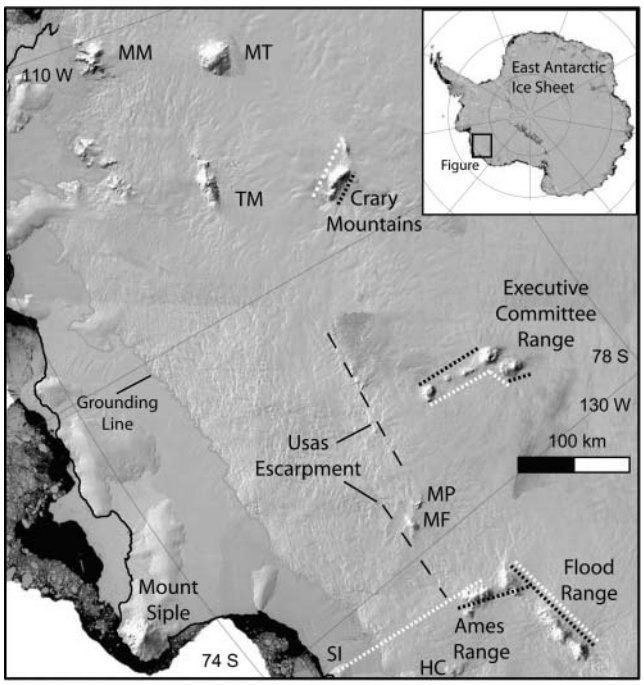

Fig. 2. Landsat Image Mosaic of Antarctica (LIMA; Bindschadler *et al*. 2008) showing the north–south and east–west volcano alignments, as well as the isolated volcano edifices in Marie Byrd Land (LIMA image from http://lima.usgs.gov/). White dotted lines are previously defined volcano chains, whereas black dotted lines are alignments defined in this paper based on volcanic ages and morphometric attributes of the volcanoes. Abbreviations as in Figure 1, and HC, Hobbs Coast; MF, Mount Flint; MP, Mount Petras; SI, Shepard Island.

relatively poor, our results point to key links between the crustal stress regime and glacial loading over the time period of volcanism and glaciation in the Marie Byrd Land sector of the West Antarctic Rift system.

Background

Palaeogene to Neogene Volcanism in Marie Byrd Land

Sparse volcanism has occurred in Marie Byrd Land since *c*. 36 Ma, but more voluminous and widespread eruptive activity began in the Miocene at about 14 Ma (LeMasurier & Rex 1989; Wilch & McIntosh 2000; Fig. 4). Eighteen major polygenetic shield and stratovolcanoes, which incorporate 26 major vent edifices, and numerous smaller monogenetic cones and flows have formed from the mid-Miocene to the present (Figs 1 and 2; LeMasurier & Thomson 1990). The volcanic rocks rest unconformably on underlying Palaeozoic metamorphic and intrusive rocks that are intruded by Cretaceous granites; the unconformities in each isolated nunatak have been inferred to be a single, regional surface, termed 'the West Antarctic Erosion Surface' (LeMasurier & Landis 1996), although direct age constraints to confirm this hypothesis are lacking. The majority of the polygenetic volcanoes in Marie Byrd Land are not randomly distributed, but instead occur within roughly linear volcano chains (Fig. 2). LeMasurier & Rex (1989) interpreted a rectilinear pattern defined by roughly north–south and subperpendicular roughly east–west volcano chains (Fig. 2) and this remains the standard view of volcano alignments in Marie Byrd Land. Isotopic ages (K–Ar and Ar–Ar) suggested temporal progressions of volcanism along the volcano chains, from south to north in the Ames Range (Fig. 5), from east to west in the

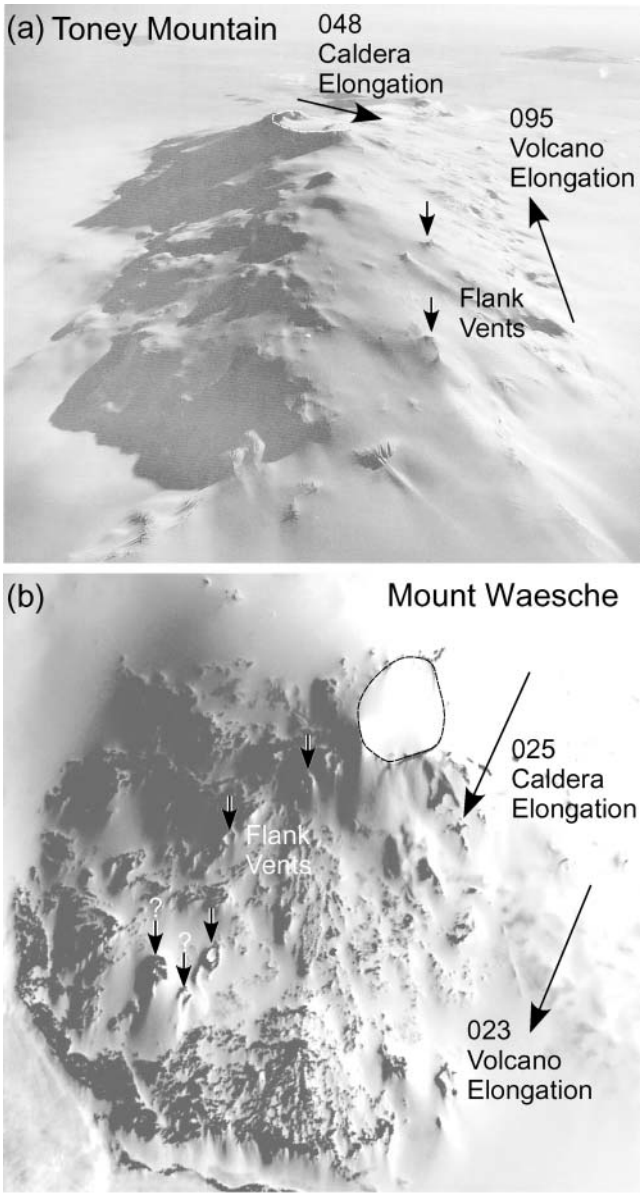

Fig. 3. (**a**) Oblique aerial photograph of the highly elongate Toney Mountain volcano with flank vents and an elongate summit caldera (from LeMasurier & Thomson 1990). (**b**) ASTER image (15 m resolution) of an elongate summit caldera and flank vents on the southern flank of Mount Waesche in the Executive Committee Range.

Flood Range (Fig. 5), and from north to south in the Executive Committee Range (Fig. 6) and the Crary Mountains (Fig. 7; LeMasurier & Rex 1989; Panter *et al*. 1994; Wilch 1997). The apparent opposing progression directions were interpreted to mark migration of magmatism away from an upwelling mantle plume centred beneath Marie Byrd Land (LeMasurier & Rex 1989). Solitary volcanoes in Marie Byrd Land occur outside the volcano chains and range in age from the Late Miocene (Mount Murphy, Mount Flint) to Pleistocene (Mount Siple, Mount Takahe, Toney Mountain) (Figs 8 and 9; LeMasurier & Thomson 1990). Here we re-evaluate both the volcano alignments and volcanic age progressions in the Marie Byrd Land region.

Marie Byrd Land rift structure

At a regional scale, the West Antarctic Rift system is a wide rift system similar in scale to the Basin and Range Rift of North America (Fitzgerald *et al*. 1986; Tessensohn & Wörner 1991). Marie Byrd Land appears to constitute an integral part of the Cretaceous West Antarctic Rift system, as evidenced by extensional crustal structures and thinned crust (Winberry & Anandakrishnan 2004; Siddoway 2008). Extensive new chronological information, combined with field mapping and regional geophysical surveying, shows that western Marie Byrd Land underwent intracontinental extension in the Cretaceous, prior to separation of 'Zealandia' from the margin of Marie Byrd Land *c*. 80 Ma (Luyendyk 1995; Storey *et al*. 1999; Gohl 2008; Siddoway 2008). The intracontinental deformation involved dextral transtension accommodated by normal faults, deep crustal detachment faults, and by steep, conjugate strike-slip faults (Siddoway 2008). A roughly north–south-oriented *c*. 100 Ma regional dyke array is associated with this pre-breakup intracontinental extension (Siddoway 2008), whereas a spatially distinct zone of east–west mafic dykes parallel to the Marie Byrd Land continental margin, dated at *c*. 107 Ma, is interpreted to mark stretching at the onset of continental breakup (Storey *et al*. 1999). The segmented, rectilinear continental margin of Marie Byrd Land is controlled by breakup-related structures. Aerogeophysical data show that east–west-oriented bedrock lineaments and escarpments, as well as faults inferred along gravity anomaly boundaries, parallel the east–west faults related to approximately mid-Cretaceous intracontinental extension mapped in outcrop (Luyendyk *et al*. 2003). The dominant structural grain formed by Cretaceous rifting and breakup in western Marie Byrd Land is oriented east–west, with subsidiary north–south structural trends.

Recent acquisition of bedrock elevation data beneath the Amundsen Sea sector of the West Antarctic Ice Sheet, including easternmost Marie Byrd Land (Fig. 10), shows deep linear troughs oriented roughly east–west, separating elongate Neogene volcanoes that partially emerge above the ice sheet surface (Holt *et al*. 2006). The similarity in the 'basin-and-range' style of linear troughs and uplifted blocks, as well as the east–west orientation, is striking between western Marie Byrd Land and easternmost Marie Byrd Land. Only sparse data constrain the bedrock topography across interior Marie Byrd Land; however, there is the prominent, north-facing Usas Escarpment that traverses this region for over 300 km with an east–west trend, suggesting a linkage of the fault-block topography across the entire Marie Byrd Land region. A dominant east–west rift structure is consistent with the east–west elongate shape of the Marie Byrd Land block as a whole (Fig. 1). Marie Byrd Land may also constitute the uplifted northern flank of the Cenozoic West Antarctic Rift system, which lies inboard beneath the West Antarctic Ice Sheet (LeMasurier 1990; Behrendt *et al*. 1994; LeMasurier 2008).

LeMasurier & Rex (1989) argued for *c*. 25 Ma and younger doming and fault-block displacement in Marie Byrd Land based on the elevation pattern of erosional contacts between Palaeozoic–Mesozoic basement rocks and overlying Palaeogene and Neogene volcanic rocks. This interpretation assumes a single, province-wide erosional surface, that this surface originally formed at sea level, and that the erosional surface was nearly horizontal and hence forms a marker horizon (LeMasurier & Rex 1983). Luyendyk *et al*. (2001) argued that the regional erosion surface in Marie Byrd Land could have formed at higher elevation and be of Cretaceous age, coeval with documented extension and uplift. Wilch & McIntosh (2000) documented over

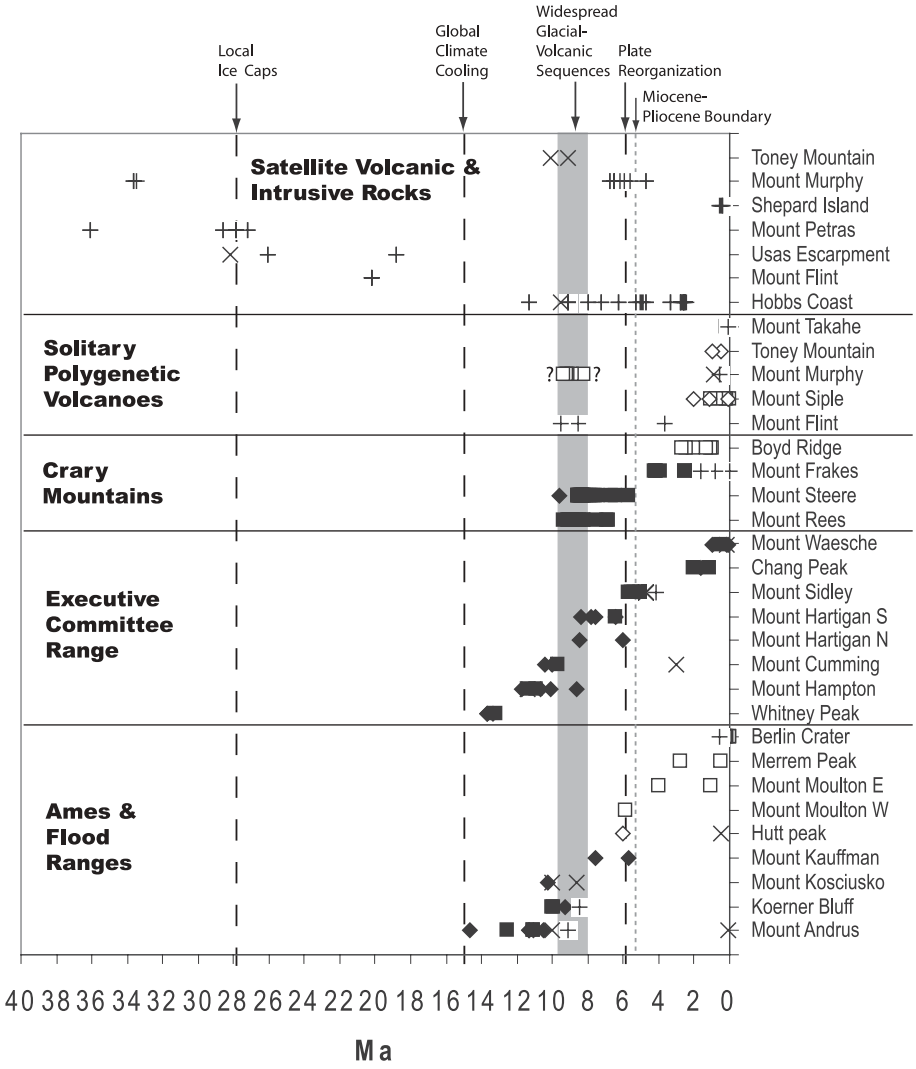

Fig. 4. Plot showing K–Ar (diamond and × symbols) and Ar–Ar (square and + symbols) ages for volcanic rocks forming polygenetic volcanoes and isolated vents in Marie Byrd Land volcanic province. Significant time points in the development of the West Antarctic Ice Sheet and timing of a Late Miocene plate reorganization are indicated. K–Ar ages are not reported in cases where there has been significant revision of volcanic ages by more recent Ar–Ar age analyses in the same area. White boxes and diamonds show east–west volcanism, whereas black boxes and diamonds show north–south volcanism. Question marks by Mount Murphy white boxes reflect questionable east–west volcano elongation data. Symbols × and + show ages for volcanic and intrusive rocks that are not clearly associated with the main phases of polygenetic volcanism that created the volcano edifices (e.g. monogenetic vents). Ages compiled from LeMasurier & Thomson (1990), Panter *et al*. (1994), Wilch (1997), Wilch *et al*. (1999), Wilch & McIntosh (2000, 2002, 2007). The locations of Hobbs Coast and Siple Island are shown in Figure 2.

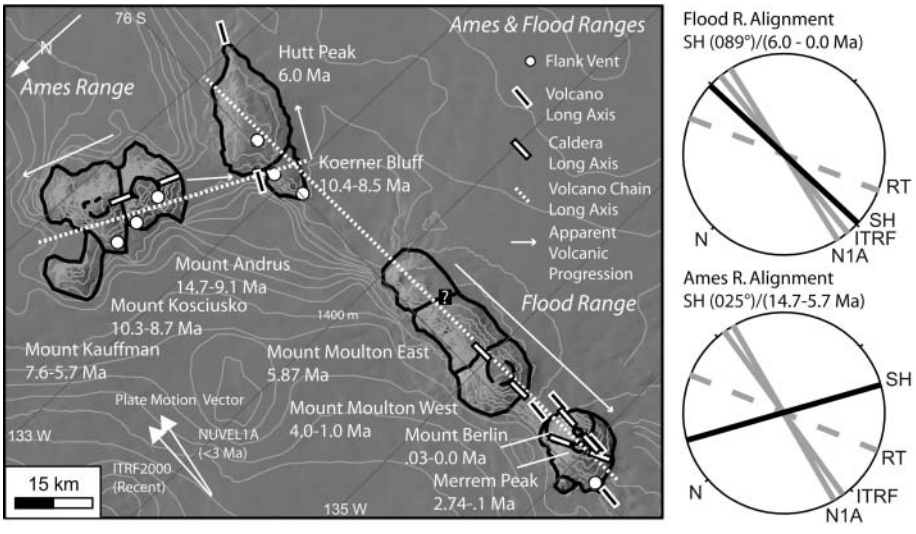

Fig. 5. LIMA image showing major volcanoes, cinder cones (open circles), and calderas associated with the north–south and east–west volcano chains of the Ames and Flood ranges. Major calderas have long axes parallel to the north–south (Mount Andrus) and east–west (Mount Moulton West, Merrem Peak, and Berlin Crater volcanoes) alignments of volcanoes. Plate motion directions from NUVEL1A (last 3 Ma) and measured by global positioning system (GPS) (ITRF2000, present) are shown by white arrows. Volcanism prior to 6.0 Ma predominantly occurred in the Ames Range, where volcanoes show a northward progression of volcanism from Mount Andrus to Mount Kauffman and a coeval southward progression of volcanism to Koerner Bluff volcano. Volcanism since ≤6.0 Ma has predominantly occurred in the Flood Range, where it progressed from east to west. Rose diagrams show interpreted S_H directions with respect to present plate motion and calculated ridge torque directions.

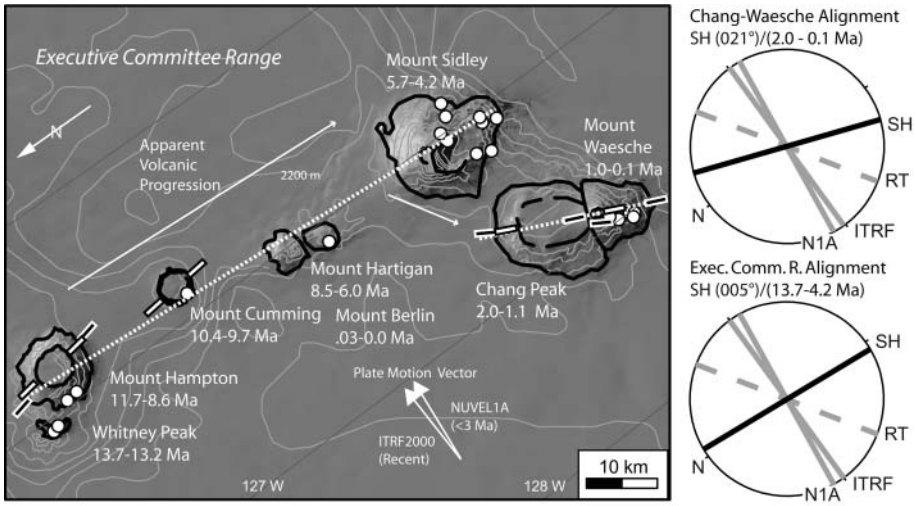

Fig. 6. LIMA image showing major volcanoes, cinder cones (open circles), and calderas associated with the north–south volcano chain of the Executive Committee Range. Plate motion directions from NUVEL1A (last 3 Ma) and measured by GPS (ITRF2000, present) are shown by white arrows. Volcanism progressed from north to south from Whitney Peak to Mount Sidley. Younger Plio-Pleistocene volcanism progressed from NNE to SSW along Chang Peak and Mount Waesche. Rose diagrams show interpreted S_H directions with respect to present plate motion and calculated ridge torque directions. Symbols are as in Figure 5.

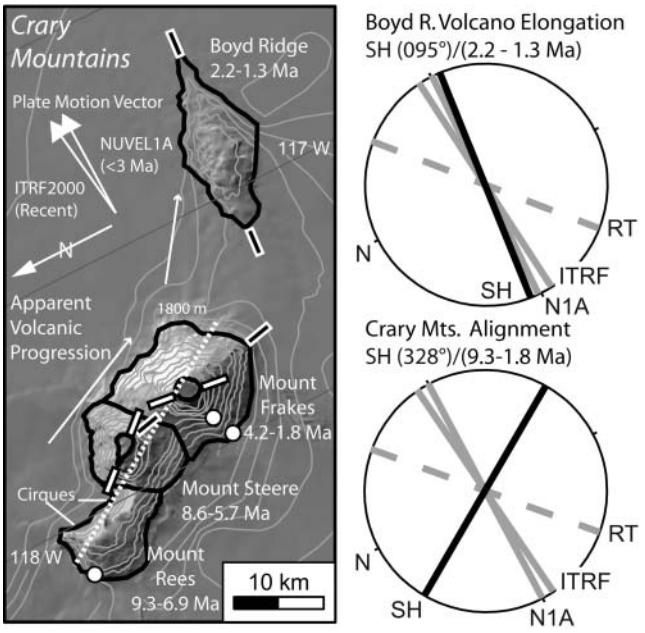

Fig. 7. LIMA image showing major volcanoes, cinder cones (open circles), and calderas associated with the NW–SE volcano chain of the Crary Mountains. Plate motion directions from NUVEL1A (last 3 Ma) and measured by GPS (ITRF2000, present) are shown by white arrows. Volcanism progressed from NW to SE from Mount Rees to Mount Frakes. Younger volcanism occurred to the east at Boyd Ridge. Rose diagrams show interpreted S_H directions with respect to present plate motion and calculated ridge torque directions. Symbols are as in Figure 5.

400 m of relief on the erosional unconformity, indicating that the erosion surface did not have uniform initial elevation. Other than the inferred offset of the erosional unconformity, evidence of 'block faulting' consists of north–south and east–west rectilinear margins of coastal nunataks (LeMasurier & Rex 1983) and the apparent relative displacement of horst-like glacial interfluves and graben-like glacial valleys (Wilch & McIntosh 2007). A Neogene age for this inferred faulting is derived from the pattern of older volcanic rocks on higher-elevation erosion surfaces and younger volcanic rocks on lower-elevation erosion surfaces, interpreted as circumferential rise of 'fault-blocks' through time (LeMasurier & Rex 1989). LeMasurier (2008) argued that the basins of the West Antarctic rift system, south of Marie Byrd Land in the Antarctic interior, developed by rifting beneath the West Antarctic Ice Sheet during the Neogene, based on the low elevation, isostatic disequilibrium, and lack of sediment fill characterizing the basins. No faults are observed to cut the Neogene volcanoes that emerge above the ice sheet, the only young stratigraphic markers exposed in Marie Byrd Land. Although there is mainly indirect evidence for Neogene faulting in Marie Byrd Land, without further data it cannot be ruled out.

Polygenetic volcanoes as stress indicators

Volcano alignments

Narrow alignments of polygenetic volcanoes are common on the Earth's surface. They can range in length from tens of kilometres on the continents (e.g. Barberi & Varet 1977) to hundreds of kilometres in the ocean basins (e.g. Jackson & Shaw 1975) and are distinct from the broad linear or curvilinear arcs of volcanoes that form as a result of lithospheric rifting and subduction (Nakamura *et al*. 1977). Polygenetic volcano alignments have been suggested to form as a result of movement of the lithosphere over a stationary hotspot (Morgan 1971), and by the exploitation of pre-existing or magmatically induced fractures by magmatism (Turcotte & Oxburgh 1973; Jackson & Shaw 1975; Favela & Anderson 1999; Sandwell & Fialko 2004; Natland & Winterer 2005; Foulger 2007). In cases where hotspot magmatism can be ruled out for reasons such as a lack of a clear temporal progression of volcanism (e.g. Richardson *et al*. 1979; McNutt *et al*. 1997), volcano chains are likely to have formed along magmatically induced or pre-existing fractures that are favourably oriented with respect to the stress field in the plate (Favela & Anderson 1999). Unlike monogenetic cinder cone alignments that form contemporaneously along a single feeder dyke or fissure, polygenetic volcanoes form by eruptions from a multitude of feeder dykes distributed around a central magma conduit. Stress and structurally controlled polygenetic volcano chains do not necessarily erupt contemporaneously, but their narrow alignment indicates that they are likely to have ascended

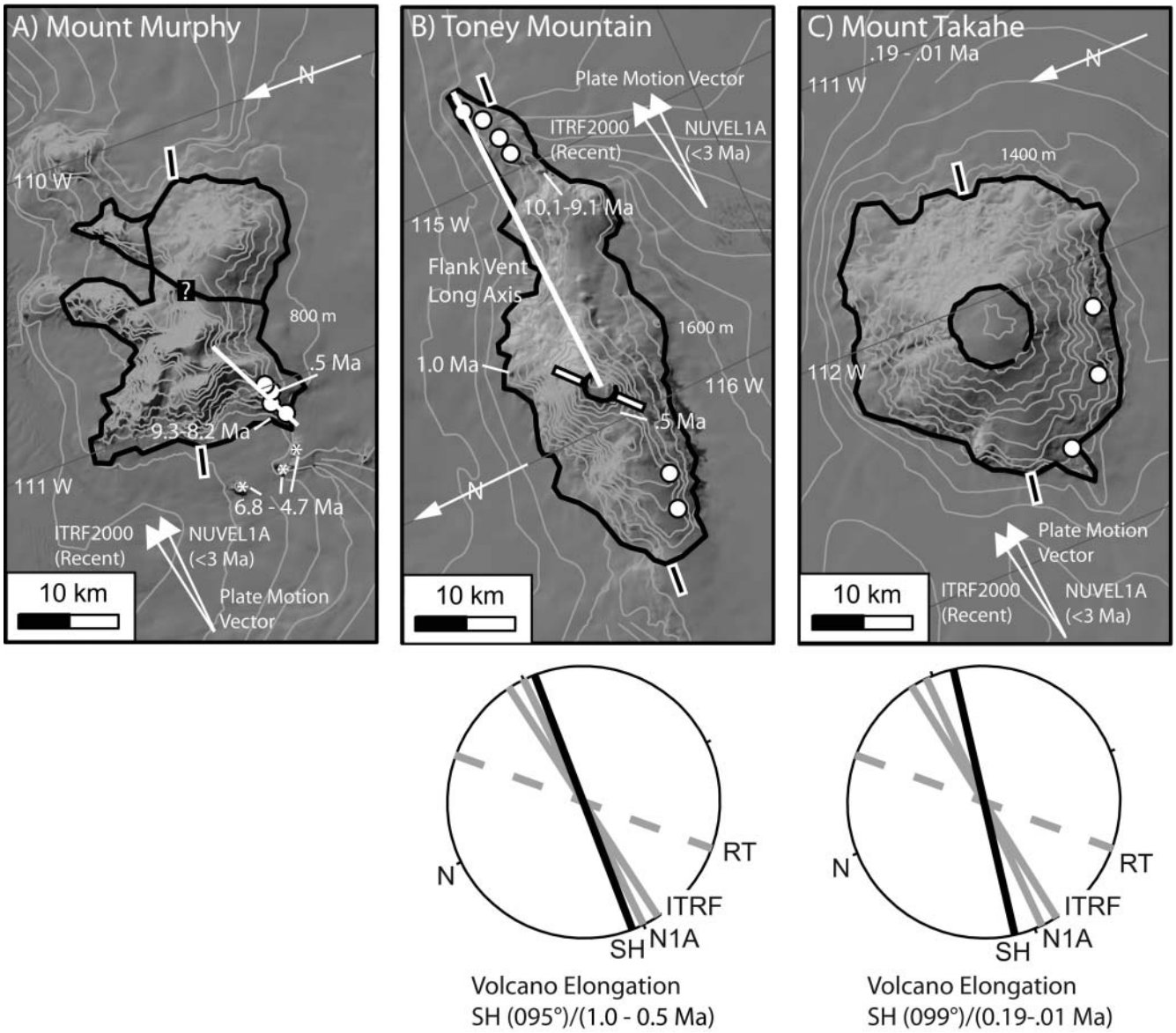

Fig. 8. LIMA images showing major solitary elongate volcanoes in the eastern sector of Marie Byrd Land: (**a**) Mount Murphy, (**b**) Toney Mountain, and (**c**) Mount Takahe, with associated cinder cones (open circles) and calderas. Plate motion directions from NUVEL1A (last 3 Ma) and measured by GPS (ITRF2000, present) are shown by white arrows. Rose diagrams show interpreted S_H directions with respect to present plate motion and calculated ridge torque directions for Toney Mountain and Mount Takahe.

along similarly striking and/or genetically linked magmatically induced or pre-existing fracture systems (Kear 1964; Foulger 2007). New fractures formed as magmatic hydrofractures are parallel to the maximum horizontal stress (S_H) and perpendicular to the minimum horizontal stress (S_h) directions (Anderson 1951). The direction of hydrofracture propagation can change as a result of local factors such as changes in material properties and the proximity to magma chambers (Gudmundsson 2009), but such fractures are commonly vertical in the crust because of the typical horizontal and vertical orientations of principal stresses in the crust. Existing fractures may also be exploited by magmatism, but such fractures must be subperpendicular to the S_h direction, or else it would be more efficient for magmatic pressures to form a new tensile fracture (Delaney *et al*. 1986). Therefore, the trend of the volcano chains yields a first-order estimate of the maximum horizontal stress direction at the time the alignment formed, at least where a hotspot mechanism can be ruled out. A structural control on volcanism can be confirmed by comparison of bedrock structural trends with the directions of volcano shape elongation, flank vent eruptions, and elongate summit calderas, which we review below.

Elongate volcanoes and flank vent distributions

Nakamura (1977) outlined a technique to determine palaeostress directions using the elongated shapes of volcanoes and the orientation of elliptical zones of monogenetic volcanoes on polygenetic volcano flanks (Fig. 11). Magmatically induced hydrofracturing of the volcanic edifice forms subsurface feeder dykes marked at the surface by linear arrays of monogenetic

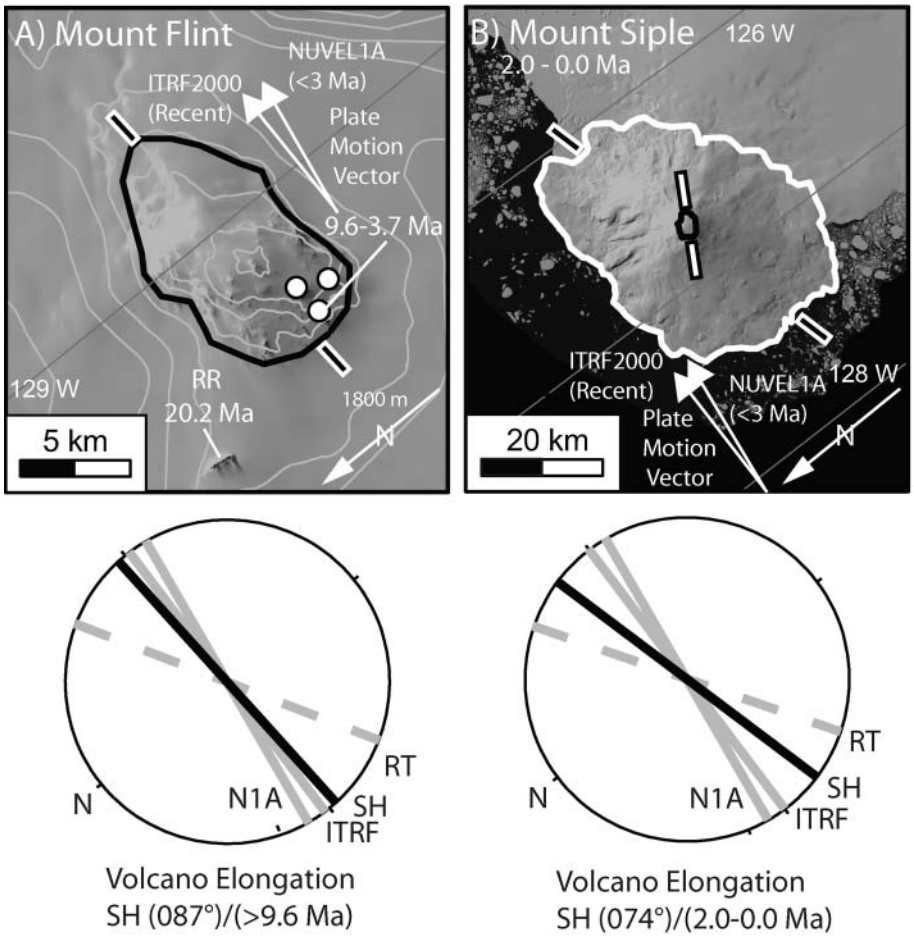

Fig. 9. LIMA images showing major solitary elongate volcanoes in the central and northern sectors of Marie Byrd Land: (**a**) Mount Flint and (**b**) Mount Siple, with associated cinder cones (open circles) and calderas. Plate motion directions from NUVEL1A (last 3 Ma) and measured by GPS (ITRF2000, present) are shown by white arrows. Rose diagrams show interpreted S_H directions with respect to present plate motion and calculated ridge torque directions.

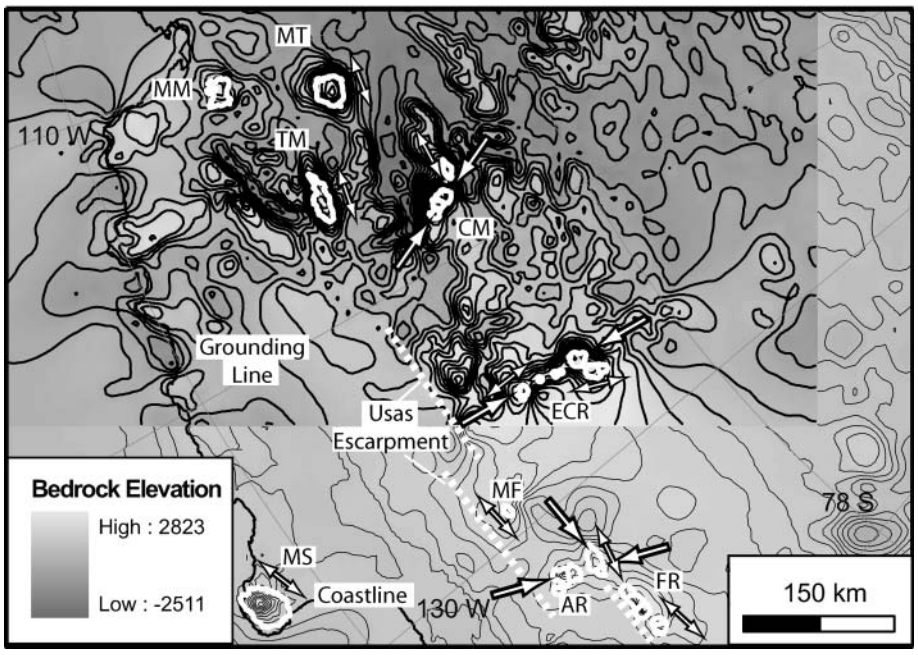

Fig. 10. Bed elevation map showing subglacial bedrock topography in Marie Byrd Land. The higher resolution data in eastern Marie Byrd Land show prominent east–west linear 'basin-and-range' type bedrock topography. The east–west-trending bedrock ridges below the Toney Mountain, Mount Takahe, and Mount Murphy volcanoes, parallel to the east–west volcano elongation directions (double-ended white arrows), should be noted. Volcano alignments are shown with thick white arrows. Central Marie Byrd Land is covered by only lower resolution bedrock elevation data. Bed elevation data from Lythe *et al*. (2000) and Holt *et al*. (2006). Abbreviations are as in Figure 1.

volcanoes. Magmatic hydrofractures initiate near the central conduit of a volcano, then propagate laterally and vertically outward and assume the direction of the regional S_H direction (Nakamura 1977; Gudmundsson 2006). Surface vents align along the subsurface trace of the dyke (Nakamura 1977; Nakamura *et al*. 1977), thus lines connecting the main polygenetic volcano edifice to flank vents track the radial dykes. Dykes preferentially form and extend for greater distances in the S_H direction, so the

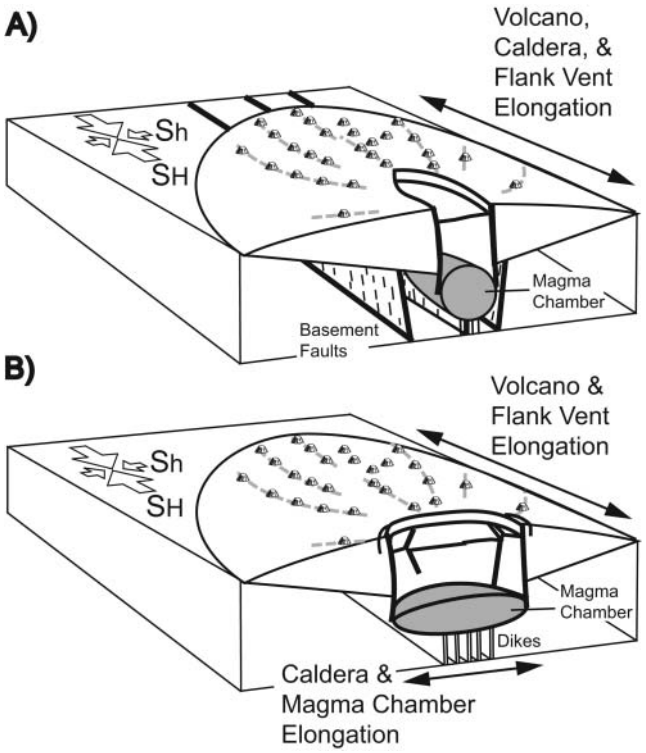

Fig. 11. Schematic models depicting volcano elongation, elongated flank vent distribution, magma chamber elongation, and summit caldera elongation patterns on polygenetic volcanoes formed under a differential stress field. Dykes and fissures preferentially trend parallel to the S_H direction, producing elongated vent fields and elongate volcanic edifices. Summit calderas (and their underlying magma chambers) may be elongate parallel to the volcano elongation direction (and the S_H direction) when magmatism is structurally controlled by crustal fractures that strike at a high angle to the S_h direction (**a**). Summit calderas can be elongate perpendicular to the volcano elongation and parallel to the S_h direction (similar to borehole breakouts) as a result of stress field control on magma chamber growth and/or caldera ring fracture dip (**b**).

long axis of their elliptical distribution serves as a proxy for the S_H direction. The preferred dyke orientation formed under differential stress conditions causes the elongation of a polygenetic volcano, which provides an auxiliary means for determining the S_H direction (Nakamura 1977). Elongate volcanoes can also develop parallel to S_H in cases where they form above extension fractures in the crust (Adiyaman *et al*. 1998).

Elongate summit calderas

Fractures within the crust can control magma chamber growth (Acocella *et al*. 2002; Acocella 2006), producing elongate magma chambers and calderas parallel to the volcano elongation direction and at a high angle to the extension or S_H direction (Fig. 11a; Nakamura 1977; Holohan *et al*. 2005). Alternatively, elongation of summit calderas can form because magma conduits have circumferential stress concentrations similar to fluid-filled boreholes and can thus develop breakouts that elongate the collapsing caldera in the direction of S_h (Fig. 11b) (Bosworth *et al*. 2003; Holohan *et al*. 2005). Although additional factors such as asymmetric subsidence can influence caldera shapes (Holohan *et al*. 2005), stress or structural control on caldera elongation direction can be assessed by comparison with other independent stress data such as the trend of volcano chains, as well as volcano elongation and flank vent directions.

Flank vent, volcano, and caldera shape analysis

Methods

LeMasurier & Rex (1989) defined a rectilinear pattern of volcano chains in Marie Byrd Land. Their volcano chains consist of both closely spaced volcanoes and isolated volcanoes separated by large distances from the main 'chain' (Fig. 2), and many of their chains include volcanoes of widely different ages. For example, LeMasurier & Rex (1989) interpreted some satellite volcanism at Shepard Island as marking the early stages of shield volcano development, and included this minor volcanic centre within their north–south Ames Range volcano chain (Fig. 2), despite the large distance from the main chain (*c*. 135 km), and the widely different age (a 6 Ma difference) of Shepard Island volcanism (Pleistocene) with respect to the polygenetic volcanism in the Ames Range (Miocene). Here we take a different approach by mapping polygenetic volcano alignments where volcanoes are in close proximity and have a limited age range. We use two relatively broad time windows separated by the Miocene–Pliocene boundary (*c*. 5.3 Ma, Gradstein *et al*. 2004) to assess any changes in volcanic alignments or volcano elongations through the Neogene.

We mapped the shapes of the polygenetic volcanoes, the locations of flank vents, and the shapes of summit calderas using a combination of existing maps (González-Ferrán & González-Bonorino 1972; LeMasurier & Thomson 1990; Panter *et al*. 1994; Wilch 1997; Smellie 2001), Landsat satellite imagery (Figs 5–9; 30 m ground resolution), and aerial photography. For our base map, we used the Landsat Image Mosaic of Antarctica (LIMA; Bindschadler *et al*. 2008), which has provided the first seamless, relatively detailed views of the polygenetic volcanoes and their summit calderas. We determined the long axis orientation and the axial ratio (long axis/short axis) for the shapes of the polygenetic volcanoes, the flank vent distributions, and any summit calderas. Axial ratios $\geqslant$1.1 were required to be classified as elongate.

The reliability of the shapes of polygenetic volcanoes, flank vent distributions, and summit calderas was assigned rankings of definite (A rank), probable (B rank), possible (C rank), and unreliable or indeterminate (D rank) (Table 1). Uncertainty in the shape of a volcano is due to low axial ratio, erosion of the edifice, snow cover, and volcano coalescence, which typically led to an unreliable rating unless contour lines defined a clear volcano shape (e.g. the Berlin Crater volcano, Fig. 5). Uncertainty in flank vent azimuths is due to low vent numbers, such that azimuths are highly dependent on single cones, or to flank vents being restricted to a single volcano flank. Uncertainty in summit caldera azimuths is due to low axial ratio, incomplete caldera rims, and lack of physiographic expression of rims on the Landsat imagery. Table 1 lists the azimuths, axial ratios, ages, and reliability rankings of all of the volcanoes, flank vents, and summit calderas. In the sections below, we restrict our analysis to the most reliable data (A and B reliability ranks).

The age of polygenetic and flank vent volcanism is constrained by published Ar–Ar analyses (Panter *et al*. 1994; Wilch 1997; Wilch *et al*. 1999; Wilch & McIntosh 2000, 2002, 2007) and earlier, less precise K–Ar analyses (LeMasurier & Thomson 1990), compiled for this study. The age of each caldera is taken to be the age of the youngest pre-caldera lavas. Figure 4 shows volcanic ages for Marie Byrd Land for isolated volcanic centres

Table 1. *Elongate volcanoes, flank fissures, and elongate calderas in Marie Byrd Land, Antarctica*

Volcano name	Volcano axial ratio	Volcano elongation azimuth (°)	Reliability rank	Number of flank vents	Flank vent azimuth (°)	Reliability rank	Caldera axial ratio	Caldera azimuth (°)	Reliability rank	Main edifice volcanism age (Ma)	Flank vent volcanism age (Ma)
Solitary volcanoes											
Mount Takahe	1.1	099	A	(3)	080	D	1.0	–	B	0.2–0.0	0.1
Mount Siple	1.2	074	A	0	–	–	1.5	121	B	2.0–0.0	
Toney Mountain	3.2	095	A	6	087	B	1.2	048	A	(1.0–0.5)	<9.5, <1.0–0.5
Mount Murphy	1.4	104	D	(4)	065	C	–	–	–	9.3–8.2	0.6
Mt. Flint	1.6	087	B	(3)	075	C	–	–	–	>9.6	9.6, 8.6, 3.7
Ames and Flood ranges											
Mount Berlin, Berlin Crater	1.8	088	B	0	–	–	1.3	091	A	0.03–0.0	
Mount Berlin, Merrem Peak	1.2	097	B	(1)	109	D	2.2	068	A	2.7–0.1	0.6
Mount Moulton West	1.3	003	D	0	–	–	1.1	091	B	3.9–1.0	
Mount Moulton East	2.5	092	D	–	–	–	–	–	–		
Hutt Peak	2.1	117	A	0	–	–	–	–	–	(6.0)	(0.5)
Mount Kauffman	1.2	146	D	(1)	–	–	–	–	–	(7.6–5.7)	
Koerner Bluff	1.3	090	C	(2)	077	D	–	–	–	10	(9.3), 8.4
Mount Kosciusko	1.1	108	D	(1)	104	D	1.3	018	C	(10.3–10.0)	(8.7)
Mount Andrus	1.3	118	D	(2)	146	D	1.3	018	B	(14.7–10.0)	9.2, (0.1)
Executive Committee Range											
Mount Waesche	1.6	023	B	(5)	035	C	1.3	025	A	(1.0–0.1), 0.5	(0.17)
Chang Peak	1.4	032	B	0	–	–	1.5	020	A	2.0–1.1	
Mount Sidley	1.0	–	D	(9)	008	C	1.0	–	D	5.7–4.25	4.2
Mount Hartigan S	1.3	152	D	(1)	068	D	–	–	–	(8.4)–6.4	<6.4
Mount Hartigan N	1.1	090	D	–	–	–	–	–	–	(8.5–6.0)	
Mount Cumming	1.0	–	D	(1)	067	D	1.1	175	A	(10.4)–9.7	(3.0)
Mount Hampton	1.1	168	B	(2)	104	D	1.1	172	A	(11.7–8.6)	(11.4)
Whitney Peak	?	–	D	(2)	120	D	–	–	–	(13.7)–13.2	<13.2
Crary Mountains											
Boyd Ridge	2.4	095	A	0	–	–	–	–	–	2.7–1.0	
Mount Frakes	1.1	170	B	(2)	074	D	1.2	007	B	4.2–1.8	1.6–0.03
Mount Steere	1.5	073	D	0	–	–	1.8	139	A	8.6–5.7	
Mount Rees	1.6	145	C	0	135	D	–	–	–	9.3–6.9	<6.9

Ages compiled from LeMasurier & Thomson (1990), Panter *et al*. (1994), Wilch (1997), Wilch *et al*. (1999) and Wilch & McIntosh (2000, 2002, 2007). Parentheses for vent numbers indicate that measurements were restricted to one side of the volcano. Ages are from Ar–Ar analyses with the exception of K–Ar ages indicated by parentheses.

(satellite intrusions) and for polygenetic volcanoes, grouped according to volcano chains.

Results of volcano analysis

Our time break, selected at the Pliocene lower boundary of 5.3 Ma, yielded a surprisingly good division in alignment and elongation trends of the volcanoes. Sixteen volcanoes formed in the Miocene, of which 12 occur in north–south volcano chains (Figs 5–7). Thus, Middle to Late Miocene volcanic activity predominantly occurred along roughly north–south volcano chains. Ten volcanoes formed in the Pliocene–Pleistocene time interval, of which seven form either an east–west chain (Fig. 5) or east–west-elongate solitary edifices (Figs 7–9). Two Miocene volcanoes forming part of the Flood Range east–west alignment are *c*. 6 Ma, the youngest end of Miocene volcanism. The youngest volcanism along the north–south Ames Range volcano alignment at Mount Kauffman (5.7 ± 0.5 Ma; K–Ar) is within analytical error of the age of volcanism at the east–west Flood Range alignment including Hutt Peak volcano (6.04 ± 0.24 Ma; K–Ar) and Mount Moulton East volcano (5.87 ± 0.05 Ma; Ar–Ar). These data suggest that *c*. 6 Ma may be a better time window boundary to delineate the age of north–south v. east–west volcanic alignments. With only three exceptions (Chang Peak and Mount Waesche in Fig. 6 and Mount Frakes in Fig. 7), the latest Miocene to Pleistocene volcanism occurred along east–west volcano chains and at isolated volcanoes with east–west elongation directions.

The highest-reliability shape analyses show that both volcano elongation directions and caldera elongation directions are parallel to the overall volcano alignments (Figs 5–7). In general, the flank vent distribution elongations were of low reliability and thus were of use as stress indicators in only one case. Miocene volcanoes in the NNE Executive Committee Range alignment (including the 5.7–4.2 Mio-Pliocene Sidley volcano) (Fig. 6) and NW Crary Mountains alignment (Fig. 7) have elongate volcano shapes and caldera elongations nearly parallel to the chain trend. In the Ames Range (Fig. 5), there are no high-quality volcano shape data, but one reliable caldera is subparallel to the NNE volcano chain. The latest Miocene–Pleistocene east–west Flood Range alignment (including the Hutt Peak 6.0 Ma volcano), have both caldera and volcano elongations parallel to the overall volcano chain trend (Fig. 5). The systematic parallelism points to the 'structural control' model for volcano and caldera shapes (Fig. 11a).

Based on the northeasterly orientation of both the volcano elongation and caldera elongation directions of the Mount Waesche–Chang Peak volcanic complex, we do not define an

east–west alignment at the south end of the Executive Committee Range (Fig. 6). This is supported by roughly north–south flank vent azimuths on Mount Sidley and Mount Waesche, although these have low shape reliability because of flank vents being restricted to a single volcano flank. Although there is a well-defined east–west elongation of Boyd Ridge volcano at the south end of the Crary Mountains (Fig. 7), there are no indications that it is aligned with other volcanoes in the north–south chain there, other than an overlap in age with Mount Frakes. We therefore interpret Boyd Ridge, as well as Chang Peak and Mount Waesche in the Executive Committee Range, as volcanoes outside linear volcano chains (Fig. 2). Our interpretation thus eliminates the apparent east–west 'doglegs' in volcano alignments in these volcano groups, leaving only the Flood Range defining an east–west volcano alignment.

We determined best-fit lines to volcano vent centre points by Deming regression analyses (i.e. orthogonal linear regression; Deming, 1943) to define volcano alignment trends. Volcanoes in the linear arrays defined here have low standard deviation distances from the best-fit lines of 0.97 km (Flood Range), 4.7 km (Ames Range), 2.6 km (Executive Committee Range), and 2.3 km (Crary Mountains). These standard deviation distances are small with respect to the 89.6 km (Flood Range), 44.1 km (Ames Range), 64.0 km (Executive Committee Range), and 18.5 km (Crary Mountains) chain lengths, indicating that the volcanoes are narrowly aligned and therefore likely to have ascended along similarly striking and/or genetically linked fracture systems.

Four of the 'solitary volcanoes' have reliable east–west elongation directions (Figs 8 and 9). The highest-reliability data show a very strong volcano elongation for the Pleistocene volcanoes. Bed elevation data (Fig. 10) show that Toney Mountain and Mount Takahe are pronounced east–west elongate bedrock ridges. Because the contact between volcanic rock and basement occurs at 3000 m below sea level at Toney Mountain (Bentley & Clough 1972), suggesting that the bedrock ridges represent subglacial continuation of the surface volcanoes, the bedrock contours provide strong confirmation of the east–west preferred orientation of the volcanoes. Boyd Ridge, offset from the south end of the Crary Mountains chain (Fig. 7), is interpreted here as an east–west elongated 'solitary volcano' of Pleistocene age. One 'solitary volcano' with an east–west elongation is of Late Miocene age (Mount Flint). The east–west elongation of this volcano could be due to east–west structural control (Fig. 11a) or preferentially oriented east–west feeder dykes (Fig. 11b).

Chang Peak and Mount Waesche, NNE–SSW elongated amalgamated volcanoes of Pleistocene age, offset from the south end of the Executive Committee Range (Fig. 6), have reliable volcano shape and parallel caldera elongations, but an anomalous orientation compared with the other east–west 'solitary' volcanoes.

Discussion

Stress and structural controls on polygenetic volcano chains

Two scenarios for behaviour of volcanic systems presented by Cañón-Tapia & Walker (2004) are relevant to Marie Byrd Land. These scenarios depend on the orientations of the regional stresses in the crust and the degree to which interconnectivity at reservoir depths allows lateral flow in the source region to replenish the magma conduit. For magma to reach the surface almost instantaneously upon rupture at the melt source, the least principal stress must remain horizontal and magma pressure must remain sufficient to pump the magma upward to cause eruption. In Marie Byrd Land, this applies to basaltic magmas, including the lower, basaltic foundations of polygenetic volcanoes, the low-volume scoria cones that were emplaced as a late phase on the polygenetic volcanoes, and the scattered monogenetic basalts that occur across the province (LeMasurier & Thomson 1990). Rapid recurrence of independent eruptions indicates that melt persists regionally in the mantle source area, near pressure conditions sufficient to cause rupture, but a relatively low degree of lateral interconnectivity limits the volume of each eruption episode. Another conduit can form very close to a previous one after lateral flow fed by regional melting processes re-establishes magma pressures. If recharge rates are very high, the same conduit can be ruptured again. Typically, a new conduit will form parallel to a previous one, with orientation controlled by the same regional stress orientations.

Polygenetic volcanoes form in the case where abundant melt is present in the source region, but low lateral interconnectivity impedes magma supply to the conduit and thus magma rise is arrested in the crust. Numerous rupture events at the source, driven by the suitable continuing pressure conditions of the melt, produce multiple intrusions in rapid succession that can result in convergence of intrusions upward, elevated temperature in the crust, partial melting, and formation of magma chambers within the crust. These crustal chambers supply central conduits that feed polygenetic volcanoes at the surface.

Linear volcano chains may form when two or more volcanoes that are suitably oriented in an anisotropic stress field develop intervening dykes, favouring the production of intervening magma chambers and volcanoes (Andrew & Gudmundsson 2008). A linear chain of polygenetic volcanoes can also develop if the lateral interconnectivity that guides the flow of melt at the source region has a preferred orientation as, for example, in parts of the mantle (Nicolas 1986, 1990). Crustal-penetrating shear zones are typically associated with strong fabrics that could guide magma flow laterally and/or vertically through the crust. The linear arrays of polygenetic volcanoes that are common in Marie Byrd Land (LeMasurier & Rex 1989) thus may be formed by the funnelling of melt along such pre-existing structures. It is less than satisfying that, as previously reviewed, there is no direct evidence for such structures in central Marie Byrd Land where the linear volcanic chains occur. However, if we hypothesize that central Marie Byrd Land has a structural history and rift-related shear zones as documented in western Marie Byrd Land (Siddoway 2008), this model is reasonable.

Neogene stress field in Marie Byrd Land

The roughly north–south and roughly east–west subperpendicular orientations of the Marie Byrd Land volcano chains have long been attributed to magma emplacement along reactivated pre-existing structures or faults or fractures coeval with Neogene volcanic activity in the province (e.g. LeMasurier & Rex 1989; Panter *et al*. 1994; Siddoway 2008). As discussed above, where available, structural data and bedrock topography indicate that the dominant Marie Byrd Land structural architecture in the upper crust has an east–west orientation, with subsidiary north–south trends, imprinted during Cretaceous rifting. Therefore it is possible that magma exploited these inherited rift trends to reach the surface.

Pre-existing structures can be reactivated as magma conduits

only if they are compatible with the stress regime existing at the time of emplacement. Given the typical horizontal and vertical orientations of principal stresses in the crust, subvertical structures are more likely to be reactivated. If the magma pressure driving upward migration exceeds the horizontal stress acting perpendicular to a pre-existing structure plus the tensile strength of the rock (Gudmundsson 2009), magma can open the structure as a conduit to the surface. This condition can be met in a structure of any trend if the regional stress field is close to isotropic. Keeping other factors equal, as the difference between the two horizontal stresses increases, pre-existing structures that are suitably oriented will be favoured to open and permit magma rise (Delaney *et al*. 1986; Rubin 1995). Most commonly, regional horizontal stresses are anisotropic and magma follows only structures that are essentially perpendicular to the S_h direction.

Clearly there are preferred orientations to the Marie Byrd Land volcano chains. Our analysis shows that there is also a preferred orientation of volcano elongation and caldera elongation directions. These attributes are characteristic of magma emplacement under anisotropic stress conditions. There are similar roughly north–south orientations of volcano alignments or elongations over the central Marie Byrd Land province during Middle–Late Miocene and nearly complete consistency of east–west orientations in the Plio-Pleistocene. This coherency indicates that first roughly north–south, then east–west, structures must have been strongly favoured by the regional stress field and that the volcano alignments and elongations formed approximately perpendicular to the S_h and parallel to the S_H directions at the time of emplacement (Figs 5–9). Thus, regardless of emplacement along pre-existing structures, there appears to have been a regional roughly north–south S_H direction in the Mid–Late Miocene, with the local exception of the east–west S_H direction indicated by volcano elongation at Mount Flint (Figs 12 and 13). An east–west regional S_H direction was dominant in Plio-Pleistocene time and persists at present, with the local exception of the NNE S_H direction indicated by the Chang Peak–Mount Waesche volcanoes (Figs 12 and 13). Present data do not allow us to determine whether Late Miocene volcanism occurred along E–W trends at Mount Murphy and Toney Mountain, but if this is the case, more variable S_H directions would be indicated for the Late Miocene. The change to a regionally uniform pattern of E–W S_H directions (with one exception) from *c.* 6 Ma to present is consistent with more strongly anisotropic stress conditions since 6 Ma.

Overall, the age data for the volcanoes allow for a shift from north–south to east–west alignment and elongation directions in a short time interval as early as *c*. 5–6 Ma (Fig. 4). The best constraints on the shift come from the Ames Range and Flood Range, where the 6.04 ± 0.24 Ma K–Ar age from the Hutt Peak volcano overlaps with a 5.7 ± 0.5 Ma K–Ar age from the Mount Kauffman volcano within the adjacent NNE volcano alignment, bracketing the reorientation between 5.7 and 6.0 Ma. On the Mount Frakes volcano, which appears to be an anomalously young member of a NNW volcano chain, the ages of volcanic rocks associated with volcanism from the main edifice (4.2–1.8 Ma) and from flank vents (1.6–0.03 Ma) overlap with the ages of volcanism on the nearby east–west elongated Boyd Ridge volcano (2.2–1.3 Ma). Thus, the shift from roughly north–south to east–west volcanism could have occurred later than 5–6 Ma in the Crary Mountains. Alternatively, the north–south elongation of the Frakes caldera could be parallel to S_h, consistent with the coeval Boyd Ridge trend, rather than a structurally controlled caldera elongation (see Fig. 11). If this is the case, the youngest ages for NNW-aligned volcanism on

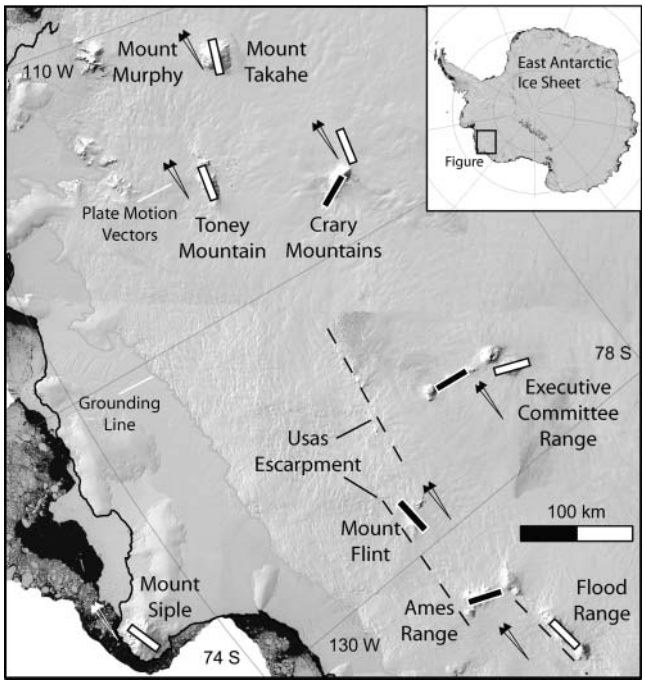

Fig. 12. LIMA image showing the S_H directions interpreted from volcano alignments, elongate volcanoes, flank vent azimuths, and elongate summit calderas in Marie Byrd Land. The dominance of east–west S_H directions for the Pleistocene (white bars) should be noted. S_H directions for Miocene volcanoes (black bars) predominantly trend north–south, except the east–west elongate Mount Flint and the possibly east–west elongate Mount Murphy.

Mount Steere (8.6–5.7 Ma) and the age of volcanism on the Mount Frakes volcano (4.2–1.8 Ma) suggest that the change in stress control occurred between 4.2 and 5.7 Ma. Exceptions to a simple stress reorientation scenario at 5–6 Ma include the Chang Peak–Mount Waesche NNE elongation of Plio-Pleistocene age, the Late Miocene Mount Flint, which has an east–west elongation, and possibly the Late Miocene Mount Murphy, with an apparent east–west elongation, but with low shape reliability because of erosion and which may be two volcanoes (J. Smellie, pers. comm.).

Origin of Neogene stress regimes

Plume control. LeMasurier & Rex (1989) suggested that a mantle plume caused doming in the centre of the Marie Byrd Land province and that volcanism migrated outward, following a north–south and east–west grid of reactivated faults, in a radial pattern linked with plume-related mantle flow. Other workers have questioned the plume origin for Marie Byrd Land volcanoes (e.g. Finn *et al*. 2005), and the timing of uplift may be older than the age of volcanism in the province (Luyendyk *et al*. 2001). The Antarctic plate has not been stationary since 80 Ma, as invoked by the plume model of LeMasurier & Rex (1989), according to palaeomagnetic (Belluso & Lanza 1996) and plate motion records (e.g. Gripp & Gordon 2002; Croon *et al*. 2008). Although the majority of the Pleistocene volcanoes do occur on the periphery of the volcanic province, in detail the volcanoes do not follow a simple younging outward pattern, as exemplified by Pleistocene Toney Mountain volcano, which occurs *c*. 150 km inside the perimeter of the volcanic province with respect to the Miocene Mount Murphy volcano (LeMasurier & Rex 1991). The

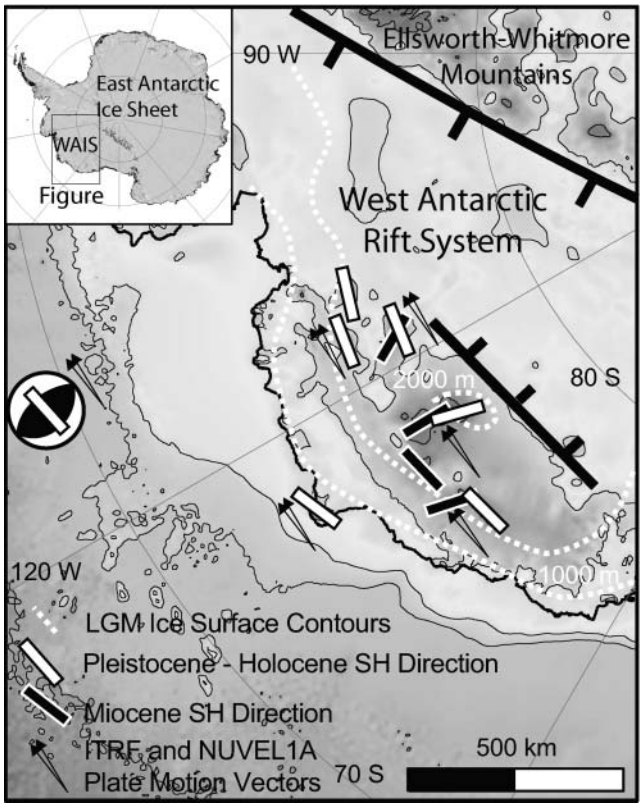

Fig. 13. Bed elevation map showing the ⩽6 Ma S_H directions from volcano alignments and elongations, as well as one offshore focal mechanism solution, with respect to the east–west elongated Marie Byrd Land area, the West Antarctic Rift system, and the Ellsworth–Whitmore Mountains. The parallelism of the S_H directions with respect to the plate motion directions, as well as the east–west elongated topography of Marie Byrd Land, should be noted. White dotted lines are reconstructed ice surface elevation contours during the Last Glacial Maximum from Denton & Hughes (2002). Inset shows the location of the figure with respect to Antarctica, as well as the location of the East and West Antarctic ice sheets. Bed elevation data from Lythe *et al*. (2000).

temporal progression of volcanism within the north–south and east–west volcano alignments is not due to movement of the Antarctic Plate over a stationary hotspot, because the age progression of volcanism in these alignments occurred in different directions over similar time periods. For example, Early to Late Miocene volcanism in the Crary Mountains and Executive Committee Range alignments shifted from north to south, whereas volcanism in the Ames Range alignment shifted both to the north and south from Mount Andrus. As discussed below, plate motion has been approximately east–west in Marie Byrd Land since the mid-Miocene. Regardless of the melting processes, we infer that regional age progressions and age patterns within chains do not support plume-related doming and mantle flow, and we therefore do not consider stress models derived from this type of doming.

Plate boundary forces. Intraplate stress fields arise from the combination of plate boundary forces with regional and/or local stress sources (e.g. Pascal & Cloetingh 2009). The World Stress Map project has shown that plate interior stress fields are commonly dominated by plate-boundary forces (Zoback *et al*. 1989). The Antarctic plate is surrounded by ridge–transform boundaries, thus the intraplate stress field should at least in part reflect the integrated 'ridge-push' forces that arise from the surrounding ridge systems. The orientation of intraplate stresses along passive continental margins and well within adjacent plate interiors is commonly parallel to the plate motion direction, consistent with 'ridge-push' forces (Zoback 1992).

Considering the young Pleistocene ages for volcanism, the east–west S_H direction is likely to represent the contemporary stress direction within the Marie Byrd Land region. This is supported by the east–west S_H direction (C quality rank) indicated by a single focal mechanism solution listed in the 2008 World Stress Map Project for a locality offshore of Marie Byrd Land (Heidbach *et al*. 2008). The east–west (+9/−16°) latest Miocene to Pleistocene S_H directions from volcano alignments and the east–west S_H from this focal mechanism solution are ⩽19° to NUVEL1A (last 3 Ma) and ⩽23° to ITRF2000 (present) plate motions. The east–west S_H directions are 18–57° from ridge torque directions modelled by Richardson (1992) (Figs 5–9 and 12). The higher angular misfits with the ridge torque directions could be due to error associated with simplification of the calculation of the ridge torque for the Antarctic plate, but are similar in magnitude to the misfits found for other plates dominated by the ridge-push force (Richardson 1992). The strong correlation between the S_H directions and the absolute plate motions indicates that the Marie Byrd Land stress field is due, at least in part, to plate boundary forces (Zoback *et al*. 1989).

Much like Africa, the Antarctic plate interior would be expected to have a compressive intraplate stress regime as a result of ridge-push forces, with areas of high topography under extension because of buoyancy forces (Zoback 1992). This relationship is borne out by the compressive thrust regime indicated by the focal mechanism solution at low elevations of the Antarctic plate offshore of Marie Byrd Land (Fig. 13). It is also consistent with the presence of linear arrays of intraplate volcanism with a horizontal least principal stress, suggesting that a normal faulting ($S_V > S_H$) or strike-slip faulting ($S_H > S_V > S_h$) stress regime characterizes the Marie Byrd Land plateau. Uniform absolute plate motions from at least 6 Ma to the present (Argus & Gordon 1991; DeMets *et al*. 1994; Gripp & Gordon 2002; Dietrich *et al*. 2004) are consistent with a regional intraplate tectonic S_H oriented east–west across Marie Byrd Land. The stage poles for Antarctic–Pacific relative plate motions were stationary from *c*. 20 to 12 Ma, then gradually tracked away from Marie Byrd Land in a progressively more northerly direction until 6 Ma, with continuing longitudinal motion to the present (Croon *et al*. 2008). Along the southwestern Pacific–Antarctic Ridge, a clockwise rotation of spreading direction of *c*. 30° since 9.7 Ma was associated with the northward migration of stage poles, and a rotation of about 8° in spreading direction occurred at *c*. 6 Ma (Cande *et al*. 1995; Croon *et al*. 2008). If the Antarctic intraplate tectonic stress field in Marie Byrd Land is dominated by the 'ridge-push' force from the nearby Pacific–Antarctic spreading centre, then no large changes in tectonic stress orientation are predicted. However, the steady east–west motion since the Late Miocene is consistent with the strongly anisotropic stress conditions and the east–west S_H direction documented here by volcano alignments in Marie Byrd Land.

The change from dominant northerly to dominant east–west volcanic chains, and interpreted S_H directions, at *c*. 6–5 Ma coincides with the timing of a major plate reorganization marked by multiple events in the Pacific basin (Cox & Engebretson 1985; Cande *et al*. 1995), including increased coupling across

the Alpine Fault in New Zealand (Cande & Stock 2004), as well as a change in plate motion along the Pacific–Antarctic Ridge (Croon *et al*. 2008). Rotations in the orientation of the crustal stress field during rifting in the Rio Grande Rift and the East African Rift have been linked to Pacific–North American plate interactions and ridge-push, respectively (Golembek *et al*. 1983; Bosworth *et al*. 1992). Using the most conservative end members of the age data for volcanism at the Mount Kauffman (5.7 ± 0.5 Ma) and Hutt Peak volcanoes (6.04 ± 0.24 Ma) in the Flood and Ames ranges, there was a 64° clockwise rotation in the S_H direction over 1.08 Ma, or *c*. 59° Ma^{-1}. This S_H rotation in Marie Byrd Land is consistent with the magnitude and rapid rates for late Pleistocene rotation in S_H direction in East Africa (Bosworth *et al*. 1992; Bosworth & Strecker 1997).

Influence of ice sheet loading on magmatism and stress regime

Glaciation and magma volumes. The terrestrial glacial record in Marie Byrd Land shows evidence for glacial ice at 29–27 Ma (Wilch & McIntosh 2000; LeMasurier & Rocchi 2005; Rocchi *et al*. 2006), and regionally extensive ice in the Oligocene appears to be consistent with the marine record (Sorlien *et al*. 2007; Miller *et al*. 2008). There is good evidence for a widespread West Antarctic Ice Sheet by *c*. 14–9 Ma (Wilch & McIntosh, 2002; Bart, 2003; LeMasurier & Rocchi, 2005) and for numerous West Antarctic Ice Sheet advances in the late Neogene (Bart & Anderson 2000; Bart 2001; Chow & Bart 2003).

Some volcanism in the Marie Byrd Land province dates back to the latest Eocene (36–34 Ma; Wilch & McIntosh 2000; Rocchi *et al*. 2006); however, more voluminous volcanic activity commenced in the Middle Miocene at 14–10 Ma (Fig. 4). Wilch & McIntosh (2002) documented a pulse of volcanism around 9–8 Ma in Marie Byrd Land, and noted that the coincidence of this pulse with the inferred first widespread glaciation could imply a causative link. Within the limits of present chronological data, there appears to be at least a rough correlation between major glacial episodes and volcanism. The initial latest Eocene–Oligocene onset of volcanism in Marie Byrd Land may be roughly coincident with, or slightly lagging behind, the initiation of glaciers, and possibly an ice sheet. Mid-Miocene onset of voluminous volcanism is approximately coeval with, or slightly lagging behind, definite establishment of a major ice sheet in Marie Byrd Land, as noted previously by Wilch & McIntosh (2002). The relatively meagre chronology available for glacial and volcanic history in Marie Byrd Land precludes evaluation of any correlation between glacial cycles and the change in stress orientation that we interpret at *c*. 6–5 Ma.

The neovolcanic zones on Iceland showed increased volcanic activity and larger volume eruptions in the late glacial and early deglacial phases of the most recent glacial cycle (e.g. Gudmundsson 1986; Sigvaldason 2002). Glazner *et al*. (1999) documented increased volcanism in the monogenetic volcanic fields of the Sierra Nevada during interglacial periods over the last 800 ka, pointing to a causative link between the glacial cycles and eruptive pulses. Jellinek *et al*. (2004) showed a correlation between volcanic pulses and deglaciation for the same region, but observed discrete lag times for basaltic and silicic volcanism. Increased volcanism upon deglaciation in Iceland and other glaciated active volcanic provinces has been attributed to the progressive changes in the stress regime affecting the crust and mantle, and the resultant influence on magma storage and transport during a loading–unloading cycle (e.g. Gudmundsson 1986; Nakada & Yokose 1992; Glazner *et al*. 1999; Andrew & Gudmundsson 2007). The imposition of a glacial load on the surface increases the magnitude of lithostatic stress at depth, which influences the critical magma pressure required to rupture the wall rocks to form a dyke and propagate it to the surface to cause an eruption. Rapid unloading as the ice sheet decays lowers the lithostatic stress, and reverses bending stresses, relaxing compressive stresses within the lithosphere and facilitating magmatic hydrofracture at depth and dyke ascent to the surface. Higher eruption volumes immediately upon deglaciation indicate that a larger amount of melt was present in the reservoir and was tapped upon unloading (Andrew & Gudmundsson 2007). Increased melt in mantle reservoirs can be related to stress-induced increase in fracture porosity and reservoir size (Andrew & Gudmundsson 2007) and/or to enhanced melting rates caused by decompression of the mantle (Jull & McKenzie 1996; Maclennan *et al*. 2002).

There are insufficient chronological data to directly link the pulses of volcanicity in Marie Byrd Land to interglacial periods. However, the apparent time coincidence of volcanism with major ice sheet development does at least suggest that stress changes related to glacial cycles have probably influenced Neogene volcanic episodes in Marie Byrd Land.

Glacial cycles and crustal stress conditions. The orientation and magnitudes of the net stresses, as well as the integrated stress regime, in the lithosphere after an ice sheet load is imposed on the surface depends on the pre-existing 'tectonic' stress orientations, magnitudes, and regime, the spatial position of a site with respect to the ice sheet centre and margins, the size and mass of the ice load, and the physical properties and rheological behaviour of the lithosphere and asthenosphere (e.g. Gudmundsson 1986; Klemann & Wolf 1998; Stewart *et al*. 2000; Andrew & Gudmundsson 2007). Isostatic stresses imposed on a purely lithostatic stress regime will cause spatial variations in compressive and tensile stresses both with depth and laterally (Klemann & Wolf 1998). Where tectonic stresses in the crust are present prior to the glacial loading–unloading cycle, the constructive or destructive 'interference' of the isostatic and tectonic stresses depends on the position with respect to the ice load (Stewart *et al*. 2000). Around the former centre of the ice load, there will be a radial pattern of decreasing uplift magnitude and of outward-directed horizontal motion toward the margins of the ice load. Reactivation of pre-existing structures, and/or the formation of new structures, is controlled by the superposition of the stresses related to isostatic motions caused by deglaciation on the orientation of tectonic stresses and on the original stress regime (extensional, thrust or strike-slip) (Muir-Wood 2000). Where tensile stresses caused by uplift upon deglaciation are parallel to the tectonic S_H direction, the horizontal stress difference will decrease and it is possible for S_H and S_h to 'flip' in direction. Where the tensile stresses are parallel to the tectonic S_h direction, stress difference increases and promotes failure, but no change in orientation of S_H and S_h will occur.

The initiation of voluminous volcanism in the Middle Miocene in Marie Byrd Land suggests that melt found 'easy' fracture pathways from the underlying reservoir beginning at this time. A net north–south S_H promoted opening of north–south pre-existing structures or dyke swarms, possibly attributable to a reduction in lithostatic stress upon deglaciation. This stress control persisted until the latest Miocene, when the preferred orientation of magmatic hydrofractures changed to an east–west orientation. The configuration of the West Antarctic Ice Sheet, at present and in reconstructions for the Last Glacial Maximum (e.g. Denton & Hughes 2002), shows a highly elongated, steep,

east–west ice margin parallel to the coast (Fig. 13). In this configuration, north–south flexural stresses governed by bending parallel to the dominant east–west margin of the ice sheet would be expected. North–south flexural stresses would be amplified by ocean loading along the east–west continental margin as ice retreated. The influence of north–south flexural tensile stress as the crust bends upward upon deglaciation would be to increase the differential stress and more strongly promote east–west-trending extension fractures if the tectonic S_H is oriented east–west, or to reduce the magnitude of S_H and potentially flip the S_H and S_h axes if the tectonic S_H is oriented north–south. Both scenarios favour east–west-trending extension fractures, therefore it is not likely that the change from north–south to east–west S_H is a result of stresses imposed by glacial loading cycles.

Conclusions

Our results provide a new definition of linear volcano chains in Marie Byrd Land by using criteria similar to those in volcanic alignment studies for stress analyses (e.g. Paulsen & Wilson 2009). Our analyses of the orientations and ages of polygenetic volcano chains, elongate volcano edifices, and elongate summit calderas in Marie Byrd Land indicate that Middle–Late Miocene volcanism occurred primarily along roughly north–south volcano alignments, whereas latest Miocene–Pleistocene volcanism had a strong east–west preferred orientation. The results are consistent with anisotropic stress conditions controlling both phases of volcanism and a rapid rotation in the maximum horizontal stress direction from north–south to east–west as early as *c*. 6 Ma. The east–west orientation of latest Miocene to Pleistocene maximum horizontal stress is parallel to the absolute motion of the Antarctic plate, suggesting that it is due, at least in part, to plate boundary forces. The stress field rotation coincides with a change in plate motion across the Pacific–Antarctic Ridge and tectonic events around the Pacific basin, indicating that the changes in the stress field reflect a major plate reorganization event. Glacial loading and unloading appears to have facilitated volcanism in Marie Byrd Land, but is unlikely to have caused this stress field rotation.

We thank A. Gudmundsson and T. Redfield for helpful reviews that improved this paper. We also thank T. Wilch, J. Smellie, K. Panter and C. Siddoway for helpful discussions on aspects of the geology of Marie Byrd Land.

References

Acocella, V. 2006. Regional and local tectonics at Erta Ale caldera, Afar (Ethiopia). *Journal of Structural Geology*, **28**, 1808–1820.

Acocella, V., Korme, T., Salvini, F. & Funiciello, R. 2002. Elliptic calderas in the Ethiopian rift: control of pre-existing structures. *Journal of Volcanology and Geothermal Research*, **119**, 189–203.

Adiyaman, O., Chorowicz, J. & Kose, O. 1998. Relationships between volcanic patterns and neotectonics in Eastern Anatolia from analysis of satellite images and DEM. *Journal of Volcanology and Geothermal Research*, **85**, 17–32.

Anderson, E.M. 1951. *The Dynamics of Faulting and Dyke Formation with Applications to Britain*, 2nd edn. Oliver & Boyd, Edinburgh.

Andrew, R.E.B. & Gudmundsson, A. 2007. Distribution, structure, and formation of Holocene lava shield in Iceland. *Journal of Volcanology and Geothermal Research*, **168**, 137–154.

Andrew, R.E.B. & Gudmundsson, A. 2008. Volcanoes as elastic inclusions: Their effects on the propagation of dykes, volcanic fissures, and volcanic zones in Iceland. *Journal of Volcanology and Geothermal Research*, **177**, 1045–1054.

Argus, D.F. & Gordon, R.G. 1991. No-net-rotation model of current plate velocities incorporating plate motion model NUVEL-1. *Geophysical Research Letters*, **18**, 2039–2042.

Barberi, F. & Varet, J. 1977. Volcanism in Afar: Small-scale plate tectonics implications. *Geological Society of America Bulletin*, **88**, 1251–1266.

Bart, P.J. 2001. Did the Antarctic ice sheets expand during the early Pliocene? *Geology*, **29**, 67–70.

Bart, P.J. 2003. Were West Antarctic ice sheet grounding events in the Ross Sea a consequence of East Antarctic ice sheet expansion during the middle Miocene? *Earth and Planetary Science Letters*, **216**, 93–107.

Bart, P.J. & Anderson, J.B. 2000. Relative temporal stability of the Antarctic ice sheets during the late Neogene based on the minimum frequency of outer shelf grounding events. *Earth and Planetary Science Letters*, **182**, 259–272.

Behrendt, J.C., LeMasurier, W.E. & Cooper, A.K. 1992. The West Antarctic rift system—A propagating rift 'captured' by a mantle plume? *In:* Yoshida, Y., Kaminima, K. & Shiraishi, K. (eds) *Recent Progress in Antarctic Earth Science*. Terra, Tokyo, 315–322.

Behrendt, J.C., Blankenship, D.D., Finn, C.A., Bell, R.E., Sweeney, R.E., Hodge, S.M. & Brozena, J.M. 1994. CASERTZ aeromagnetic data reveal late Cenozoic flood basalts (?) in the West Antarctic rift system. *Geology*, **22**, 527–530.

Belluso, E. & Lanza, R. 1996. Palaeomagnetic results from the middle Tertiary Meander Intrusives. *Antarctic Science*, **8**, 61–72.

Bentley, C.R. & Clough, J.W. 1972. Antarctic subglacial structure from seismic refraction experiments. *In:* Adie, R.J. (ed.) *Antarctic Geology and Geophysics*. Universitetsforlaget, Oslo, 683–691.

Bindschadler, R., Vornberger, P., Fleming, A., *et al.* 2008. The Landsat image mosaic of Antarctica. *Remote Sensing of Environment*, **112**, 4214–4226.

Bosworth, W. & Strecker, M.R. 1997. Stress field changes in the Afro-Arabian rift system during the Miocene to Recent period. *Tectonophysics*, **278**, 47–62.

Bosworth, W., Strecker, M.R. & Blisniuk, P.M. 1992. Integration of East African paleostress and present-day stress data: implications for continental stress field dynamics. *Journal of Geophysical Research*, **97**, 11851–11865.

Bosworth, W., Burke, K. & Strecker, M. 2003. Effects of stress fields on magma chamber stability and the formation of collapse calderas. *Tectonics*, **22**, doi:10.1029/2002TC001369.

Cande, S.C. & Stock, J.M. 2004. Pacific–Antarctic–Australia motion and the formation of the Macquarie Plate. *Geophysical Journal International*, **157**, 399–414.

Cande, S.C., Raymond, C.A., Stock, J. & Haxby, W.F. 1995. Geophysics of the Pitman fracture zone and Pacific–Antarctic plate motions during the Cenozoic. *Science*, **270**, 947–953.

Cande, S.C., Stock, J.M., Muller, R.D. & Ishihara, T. 2000. Cenozoic motion between East and West Antarctica. *Nature*, **404**, 145–150.

Cañón-Tapia, E. & Walker, G.P.L. 2004. Global aspects of volcanism: the perspectives of 'plate tectonics' and 'volcanic systems'. *Earth-Science Reviews*, **66**, 163–182.

Chow, J.M. & Bart, P.J. 2003. West Antarctic Ice Sheet grounding events on the Ross Sea outer continental shelf during the middle Miocene. *Palaeogeography, Palaeoclimatology, Palaeoecology*, **198**, 169–186.

Cooper, A.K., Davey, F.J. & Behrendt, J.C. 1987. Seismic stratigraphy and structure of the Victoria Land basin, Western Ross Sea, Antarctica. *In:* Cooper, A.J. & Davey, F.J. (eds) *The Antarctic Continental Margin: Geology and Geophysics of the Western Ross Sea*. Circum-Pacific Council for Energy and Mineral Resources, Houston, TX, 27–76.

Cox, A. & Engebretson, D. 1985. Change in motion of the Pacific plate at 5 Myr BP. *Nature*, **313**, 472–474.

Croon, M.B., Cande, S.C. & Stock, J.M. 2008. Revised Pacific–Antarctic plate motions and geophysics of the Menard Fracture Zone. *Geochemistry, Geophysics, Geosystems*, **9**, doi:10.1029/2008GC002019.

Delaney, P.T., Pollard, D.D., Ziony, J.I. & McKee, E.H. 1986. Field relations between dikes and joints: Emplacement processes and paleostress analysis. *Journal of Geophysical Research*, **91**, 4920–4938.

DeMets, C., Gordon, R.G., Argus, D.F. & Stein, S. 1994. Effect of recent revisions to the geomagnetic reversal time scale on estimates of current plate motions. *Geophysical Research Letters*, **21**, 2191–2194.

Deming, W.E. 1943. *Statistical Adjustment of Data*. Wiley, New York. (Reprinted 1964, Dover, New York.)

Denton, G.H. & Hughes, T.J. 2002. Reconstructing the Antarctic Ice Sheet at the Last Glacial Maximum. *Quaternary Science Reviews*, **21**, 193–202.

Dietrich, R., Rulke A., Ihde, J., *et al.* 2004. Plate kinematics and deformation status of the Antarctic Peninsula based on GPS. *Global and Planetary Change*, **42**, 313–321.

Favela, J. & Anderson, D.L. 1999. Extensional tectonics and global volcanism. *In:* Boschi, E., Ekstrom, G. & Morelli, A. (eds) *Problems in Geophysics for the New Millennium*. Editrice Compositori, Bologna, 463–498.

Finn, C.A., Muller, R.D. & Panter, K.S. 2005. A Cenozoic diffuse alkaline magmatic province (DAMP) in the southwest Pacific without rift or plume origin. *Geochemistry, Geophysics, Geosystems*, **6**, doi:10.1029/2004GC000723.

Fitzgerald, P.G., Sandiford, M., Barrett, P.J. & Gleadlow, A.J.W. 1986. Asymmetric extension associated with uplift and subsidence in the Transan-

tarctic Mountains and Ross Embayment. *Earth and Planetary Science Letters*, **81**, 67–78.

Foulger, G.R. 2007. The 'plate' model for the genesis of melting anomalies. *In:* Foulger, G.R. & Jurdy, D.M. (eds) *Plates, Plumes, and Plenetary Processes*. Geological Society of America, Special Papers, **430**, 1–28.

Glazner, A.F., Manley, C.R., Marron, J.S. & Rojstaczer, S. 1999. Fire or ice: anticorrelation of volcanism and glaciation in California over the past 800,000 years. *Geophysical Research Letters*, **26**, 1759–1762.

Gohl, K. 2008. Antarctica's continent–ocean transitions: consequences for tectonic reconstructions. *In:* Cooper, A.K., Barrett, P.J., Stagg, H., Storey, B., Stump, E., Wise, W. & 10th ISAES Editorial Team (eds) *Antarctica: A Keystone in a Changing World, Proceedings of the 10th International Symposium on Antarctic Earth Sciences*. National Academies Press, Washington, DC, 29–38.

Golembek, M.P., McGill, G.E. & Brown, L. 1983. Tectonic and geologic evolution of the Espanola Basin, Rio Grande Rift: Structure, rate of extension, and relation to the state of stress in the western United States. *Tectonophysics*, **94**, 483–507.

González-Ferrán, O. & González-Bonorino, F. 1972. The volcanic ranges of Marie Byrd land between long. 100° and 140°W. *In:* Adie, R.J. (ed.) *Antarctic Geology and Geophysics*. Universitetsforlaget, Oslo, 261–275.

Gradstein, F.M., Ogg, J.G., Smith, A.G., *et al.* 2004. *A Geologic Time Scale 2004*. Cambridge University Press, Cambridge.

Gripp, A.E. & Gordon, R.G. 2002. Young tracks of hotspots and current plate velocities. *Geophysical Journal International*, **150**, 321–361.

Gudmundsson, A. 1986. Mechanical aspects of postglacial volcanism and tectonics of the Reykjanes Peninsula, Southwest Iceland. *Journal of Geophysical Research*, **91**, 12711–12721.

Gudmundsson, A. 2006. How local stresses control magma-chamber ruptures, dyke injections, and eruptions in composite volcanoes. *Earth-Science Reviews*, **79**, 1–31.

Gudmundsson, A. 2009. Toughness and failure of volcanic edifices. *Tectonophysics*, **471**, 27–35.

Heidbach, O., Tingay, M., Barth, A., Reinecker, J., Kurfess, D., & Müller, B. 2008. The 2008 release of the World Stress Map. World Wide Web Address: www.world-stress-map.org.

Henrys, S. A., Wilson, T.J., Whittaker, J.M., Fielding, C., Hall, J. M. & Naish, T. 2007. Tectonic history of mid-Miocene to present southern Victoria Land Basin, inferred from seismic stratigraphy in McMurdo Sound, Antarctica. *In:* Cooper, A.K., Raymond, C.R., *et al.* (eds) *Antarctica: A Keystone in a Changing World—Online Proceedings of the 10th ISAES*. US Geological Survey Open-File Report **2007-1047**, Short Research Paper **049**; doi:10.3133/of2007-1047.srp049.

Holohan, E.P., Troll, V.R., Walter, T.R., Munn, S., McDonnell, S. & Shipton, Z.K. 2005. Elliptical calderas in active tectonic settings: an experimental approach. *Journal of Volcanology and Geothermal Research*, **144**, 119–136.

Holt, J.W., Blankenship, D.D., Morse, D.L., *et al.* 2006. New boundary conditions for the West Antarctic Ice Sheet: Subglacial topography of the Thwaites and Smith glacier catchments. *Geophysical Research Letters*, **33**, L09502, doi:10.1029/2005GL025561.

Jackson, E.D. & Shaw, H.R. 1975. Stress fields in the central portions of the Pacific Plate: Delineated in time by linear volcanic chains. *Journal of Geophysical Research*, **80**, 1861–1874.

Jellinek, A.M., Manga, M. & Saar, M.O. 2004. Did melting glaciers cause volcanic eruptions in eastern California? Probing the mechanics of dike formation. *Journal of Geophysical Research*, **109**, B09206, 10.1029/2004JB002978.

Jull, M. & McKenzie, D. 1996. The effect of deglaciation on mantle melting beneath Iceland. *Journal of Geophysical Research*, **101**, 21815–21828.

Kear, D. 1964. Volcanic alignments North and West of New Zealand's central volcanic region. *New Zealand Journal of Geology and Geophysics*, **7**, 24–44.

Klemann, V. & Wolf, D. 1998. Modelling of stresses in the Fennoscandian lithosphere induced by Pleistocene glaciations. *Tectonophysics*, **294**, 291–303.

LeMasurier, W.E. 1990. Late Cenozoic volcanism on the Antarctic plate—An overview. *In:* LeMasurier, W.E. & Thomson, J.W. (eds) *Volcanoes of the Antarctic Plate and Southern Oceans*. American Geophysical Union, Antarctic Research Series, **48**, 1–19.

LeMasurier, W.E. 2008. Neogene extension and basin deepening in the West Antarctic rift inferred from comparisons with the East African rift and other analogs. *Geology*, **36**, 247–250.

LeMasurier, W.E. & Landis, C.A. 1996. Mantle plume activity recorded by low-relief erosion surfaces in West Antarctica and New Zealand. *Geological Society of America Bulletin*, **108**, 1450–1466.

LeMasurier, W.E. & Rex, D.C. 1983. Rates of uplift and scales of ice level instabilities recorded by volcanic rocks in Marie Byrd land, West Antarctica. *In:* Oliver, J.L., James, R.R. & Jago, J.B. (eds) *Antarctic Earth Sciences*. Cambridge University Press, Cambridge, 663–670.

LeMasurier, W.E. & Rex, D.C. 1989. Evolution of linear volcanic ranges in Marie Byrd Land, West Antarctica. *Journal of Geophysical Research*, **94**, 7223–7236.

LeMasurier, W.E. & Rex, D.C. 1991. Tectonic significance of linear volcanic ranges in Marie Byrd land in late Cenozoic time. *In:* Thomson, M.R.A., Crame, J.A. & Thomson, J.W. (eds) *Geological Evolution of Antarctica*. Cambridge University Press, Cambridge, 531–532.

LeMasurier, W.E. & Rocchi, S. 2005. Terrestrial record of post-Eocene climate history in Marie Byrd Land, West Antarctica. *Geografiska Annaler*, **87**, 51–66.

LeMasurier, W.E. & Thomson, J.W. (eds) 1990. *Volcanoes of the Antarctic Plate and Southern Oceans*. American Geophysical Union, Antarctic Research Series, **48**.

Luyendyk, B.P. 1995. Hypothesis for Cretaceous rifting of east Gondwana caused by subducted slab capture. *Geology*, **23**, 373–376.

Luyendyk, B.P., Sorlien, C.C., Wilson, D.S., Bartek, L.R. & Siddoway, C.S. 2001. Structural and tectonic evolution of the Ross Sea rift in the Cape Colbeck region, Eastern Ross Sea, Antarctica. *Tectonics*, **20**, 933–958.

Luyendyk, B.P., Wilson, D.S. & Siddoway, C.S. 2003. Eastern margin of the Ross Sea Rift in western Marie Byrd Land, Antarctica: Crustal structure and tectonic development. *Geochemistry, Geophysics, Geosystems*, **4**, doi:10.1029/2002GC000462.

Lythe, M.B., Vaughan, D.G. & BEDMAP Consortium 2000. BEDMAP—bed topography of the Antarctic. 1:10 000 000 scale map. BAS (Misc) 9. British Antarctic Survey, Cambridge.

Maclennan, J., Jull, M., McKenzie, D., Slater, L. & Gronvöld, K. 2002. The link between volcanism and deglaciation in Iceland. *Geochemistry, Geophysics, Geosystems*, **3**, doi:10.1029/2001GC000282.

McNutt, M.K., Caress, D.W., Reynolds, J., Jordahl, K.A. & Duncan, R.A. 1997. Failure of plume theory to explain midplate volcanism in the southern Austral islands. *Nature*, **389**, 479–482.

Miller, K.G., Wright, J.D., Katz, M.E., Browning, J.V., Cramer, B.S., Wade, B.S. & Mizintseva, S.F. 2008. A view of Antarctic ice-sheet evolution from sea-level and deep-sea isotope changes during the Late Cretaceous–Cenozoic. *In:* Cooper, A.K., Barrett, P.J., Stagg, H., Storey, B., Stump, E., Wise, W. & 10th ISAES Editorial Team (eds) *Antarctica: A Keystone in a Changing World, Proceedings of the 10th International Symposium on Antarctic Earth Sciences*. National Academies Press, Washington, DC, 55–70.

Morgan, W.J. 1971. Convective plumes in the lower mantle. *Nature*, **230**, 42–43.

Muir-Wood, R. 2000. Deglaciation Seismotectonics: A principal influence on intraplate seismogenesis at high latitudes? *Quaternary Science Reviews*, **19**, 1399-1411.

Nakada, M. & Yokose, H. 1992. Ice age as a trigger of active Quaternary volcanism and tectonism. *Tectonophysics*, **212**, 321–329.

Nakamura, K. 1977. Volcanoes as possible indicators of tectonic stress orientation—principle and proposal. *Journal of Volcanology and Geothermal Research*, **2**, 1–16.

Nakamura, K., Jacob, K.H. & Davies, J.N. 1977. Volcanoes as possible indicators of tectonic stress orientation—Aleutians and Alaska. *Pure and Applied Geophysics*, **115**, 87–112.

Natland, J.H. & Winterer, E.L. 2005. Fissure control on volcanic action in the Pacific. *In:* Foulger, G.R., Natland, J.H., Presnall, D.C. & Anderson, D.L. (eds) *Plates, Plumes and Paradigms*. Geological Society of America, Special Papers, **388**, 687–710.

Nicolas, A. 1986. A melt extraction model based on structural studies in mantle peridotites. *Journal of Petrology*, **27**, 999–1022.

Nicolas, A. 1990. Melt extraction from mantle peridotites: Hydrofracturing and porous flow, with consequences for oceanic ridge activity. *In:* Ryan, M.P. (ed.) *Magma Transport and Storage*. Wiley, New York, 159–173.

Panter, K.S., McIntosh, W.C. & Smellie, J.L. 1994. Volcanic history of Mount Sidley, A major alkaline volcano in Marie Byrd Land, Antarctica. *Bulletin of Volcanology*, **56**, 361–376.

Pascal, C. & Cloetingh, A.P.L. 2009. Gravitational potential stresses and stress field of passive continental margins: Insights from the south-Norway shelf. *Earth and Planetary Science Letters*, **277**, 464–473.

Paulsen, T.S. & Wilson, T.J. 2009. New criteria for systematic mapping and reliability assessment of monogenetic volcanic vent alignments and elongate volcanic vents for crustal stress analyses. *Tectonophysics*, doi:10.1016/j.tecto.2009.08.025.

Reading, A.M. 2006. On seismic strain-release within the Antarctic Plate. *In:* Fütterer, D.K., Damaske, D., Kleinschmidt, G., Miller, H. & Tessensohn, F. (eds) *Antarctica*. Contributions to Global Earth Sciences, **9**, 351–356.

Richardson, R.M. 1992. Ridge forces, absolute plate motions, and the intraplate stress field. *Journal of Geophysical Research*, **97**, 11739–11748.

Richardson, R.M., Solomon, S.C. & Sleep, N.H. 1979. Tectonic stress in the

plates. *Reviews of Geophysics and Space Physics*, **17**, 981–1019.

Rocchi, S., Armienti, P., D'Orazio, M., Tonarini, S., Wijbrans, J. & Di Vincenzo, G. 2002. Cenozoic magmatism in the western Ross Embayment: role of mantle plume vs. plate dynamics in the development of the West Antarctic Rift System. *Journal of Geophysical Research*, **107**, doi:10.1029/2001JB000515.

Rocchi, S., LeMasurier, W.E. & Di Vincenzo, G. 2006. Oligocene to Holocene erosion and glacial history in Marie Byrd Land, West Antarctica, inferred from exhumation of the Dorrel Rock intrusive complex and from volcano morphologies. *Geological Society of America Bulletin*, **118**, 991–1005.

Rubin, A.M. 1995. Propagation of magma-filled cracks. *Annual Review of Earth and Planetary Sciences*, **23**, 287–336.

Sandwell, D. & Fialko, Y. 2004. Warping and cracking of the Pacific plate by thermal contraction. *Journal of Geophysical Research*, **109**, doi:10.1029/2004JB003091.

Siddoway, C. 2008. Tectonics of the West Antarctic rift system: New light on the history and dynamics of distributed intracontinental extension. *In:* Cooper, A.K., Barrett, P.J., Stagg, H., Storey, B., Stump, E., Wise, W. & 10th ISAES Editorial Team (eds) *Antarctica: A Keystone in a Changing World, Proceedings of the 10th International Symposium on Antarctic Earth Sciences*. National Academies Press, Washington, DC, 91–114.

Sigvaldason, G.E. 2002. Volcanic and tectonic processes coinciding with glaciation and crustal rebound: an early Holocene rhyolitic eruption in the Dyngjufjöll volcanic centre and the formation of the Askja caldera, north Iceland. *Bulletin of Volcanology*, **64**, doi:10.1007/s00445-002-0204.

Smellie, J.L. 2001. Lithofacies architecture and construction of volcanoes erupted in englacial lakes: Icefall Nunatak, Mount Murphy, eastern Marie Byrd Land, Antarctica. *In:* Riggs, N.R. & White, J.D.L. (eds.) *Volcaniclastic Sedimentation in lacustrine Settings*. Blackwell Science, Malden, MA, 9–34.

Sorlien, C.C., Luyendyk, B.P., Wilson, D.S., Decesari, R.C., Bartek, L.R. & Diebold, J.B. 2007. Oligocene development of the West Antarctic Ice Sheet recorded in eastern Ross Sea strata. *Geology*, **35**, 467–470.

Stewart, I.S., Sauber, J. & Rose, J. 2000. Glacio-seismotectonics; ice sheets, crustal deformation and seismicity. *Quaternary Science Reviews*, **19**, 1367–1389.

Storey, B.C., Leat, P.T., Weaver, S.D., Pankhurst, R.J., Bradshaw, J.D. & Kelley, S. 1999. Mantle plumes and Antarctica–New Zealand rifting: Evidence from mid-Cretaceous mafic dykes. *Journal of the Geological Society, London*, **156**, 659–671.

Sutherland, R. 2008. The significance of Antarctica for studies of global geodynamics. *In:* Cooper, A.K., Barrett, P.J., Stagg, H., Storey, B., Stump, E., Wise, W. & 10th ISAES Editorial Team (eds) *Antarctica: A Keystone in a Changing World, Proceedings of the 10th International Symposium on Antarctic Earth Sciences*. National Academies Press, Washington, DC, 115–124.

Tessensohn, F. & Wörner, G. 1991. The Ross Sea riftsystem, Antarctica: structure, evolution and analogues. *In:* Thomson, M.R.A., Crame, J.A. & Thomson, J.W. (eds) *Geological Evolution of Antarctica*. Cambridge University Press, New York, 273–277.

Turcotte, D.L. & Oxburgh, E.R. 1973. Mid-plate tectonics. *Nature*, **244**, 377–339.

Wilch, T.I. 1997. *Volcanic record of the West Antarctic ice sheet in Marie Byrd Land*. PhD thesis, New Mexico Institute of Mining and Technology, Socorro.

Wilch, T.I. & McIntosh, W.C. 2000. Eocene and Oligocene volcanism at Mount Petras, Marie Byrd Land: implications for middle Cenozoic ice sheet reconstructions in West Antarctica. *Antarctic Science*, **12**, 477–491.

Wilch, T.I. & McIntosh, W.C. 2002. *Lithofacies* analysis and $^{40}Ar/^{39}Ar$ geochronology of ice–volcano interactions at Mt. Murphy and the Crary Mountains, Marie Byrd Land, Antarctica. *In:* Smellie, J.L. (ed.) *Volcano–Ice Interaction on Earth and Mars*. Geological Society, London, Special Publications, **202**, 237–253.

Wilch, T.I. & McIntosh, W.C. 2007. Miocene–Pliocene ice–volcano interactions at monogenetic volcanoes near Hobbs Coast, Marie Byrd Land, Antarctica. *In:* Cooper, A.K., Raymond, C.R., *et al.* (eds) *Antarctica: A Keystone in a Changing World—Online Proceedings of the 10th ISAES*. US Geological Survey Open-File Report **2007-1047**, Short Research Paper **074**, doi:10.3133/of2007-1047.srp074.

Wilch, T.I., McIntosh, W.C. & Dunbar, N.W. 1999. Late Quaternary volcanic activity in Marie Byrd Land; potential $^{40}Ar/^{39}Ar$-dated time horizons in West Antarctic ice and marine cores. *Geological Society of America Bulletin*, **111**, 1563–1580.

Winberry, J. P. & Anandakrishnan, S. 2004. Crustal structure of the West Antarctic rift system and Marie Byrd Land hotspot. *Geology*, **32**, 922–980.

Zachos, J.C., Pagani, M., Sloan, L., Thomas, E. & Billups, K. 2001. Trends, rhythms, and aberrations in global climate 65 Ma to present. *Science*, **292**, 686–693.

Zoback, M.L. 1992. First- and second-order patterns of stress in the lithosphere: the World Stress Map project. *Journal of Geophysical Research*, **97**, 11703–11728.

Zoback, M.L., Zoback, M.D., Adams, J., *et al.* 1989. Global patterns of tectonic stress. *Nature*, **341**, 291–298.

Received 27 March 2009; revised typescript accepted 20 October 2009.
Scientific editing by Christophe Pascal and Tim Needham.